

# S-ADDOPT: Decentralized stochastic first-order optimization over directed graphs

Muhammad I. Qureshi<sup>†</sup>, Ran Xin<sup>‡</sup>, Soumya Kar<sup>‡</sup>, and Usman A. Khan<sup>†</sup>

<sup>†</sup>Tufts University, Medford, MA, USA, <sup>‡</sup>Carnegie Mellon University, Pittsburgh, PA, USA

## Abstract

In this report, we study decentralized stochastic optimization to minimize a sum of smooth and strongly convex cost functions when the functions are distributed over a directed network of nodes. In contrast to the existing work, we use gradient tracking to improve certain aspects of the resulting algorithm. In particular, we propose the **S-ADDOPT** algorithm that assumes a stochastic first-order oracle at each node and show that for a constant step-size  $\alpha$ , each node converges linearly inside an error ball around the optimal solution, the size of which is controlled by  $\alpha$ . For decaying step-sizes  $\mathcal{O}(1/k)$ , we show that **S-ADDOPT** reaches the exact solution sublinearly at  $\mathcal{O}(1/k)$  and its convergence is asymptotically network-independent. Thus the asymptotic behavior of **S-ADDOPT** is comparable to the centralized stochastic gradient descent. Numerical experiments over both strongly convex and non-convex problems illustrate the convergence behavior and the performance comparison of the proposed algorithm.

## I. INTRODUCTION

This report considers minimizing a sum of smooth and strongly convex functions  $F(\mathbf{z}) = \sum_{i=1}^n f_i(\mathbf{z})$  over a network of  $n$  nodes. We assume that each  $f_i$  is private to only on node  $i$  and that the nodes communicate over a directed graph (digraph) to solve the underlying problem. Such problems have found significant applications traditionally in the areas of signal processing and control [1], [2] and more recently in machine learning problems [3]–[6]. Gradient descent (**GD**) is one of the simplest algorithms for function minimization and requires the true gradient  $\nabla F$ . When this information is not available, **GD** is implemented with stochastic gradients and the resulting method is called stochastic gradient descent (**SGD**). As the data becomes large-scale and geographically diverse, **GD** and **SGD** present storage and communication challenges. In such cases, decentralized methods are attractive as they are locally implemented and rely on communication among nearby nodes.

Related work on decentralized first-order methods can be found in [7]–[12]. Of relevance is Distributed Gradient Descent (**DGD**) that converges sublinearly to the optimal solution with decaying step-sizes [7] and linearly to an inexact solution with a constant step-size [8]. Its stochastic variant **DSGD** can be found in [9], [10], which is further extended with the help of gradient tracking [13]–[15] in [12] where inexact linear convergence in addition

to asymptotic network independence are shown; see also [16]–[18] and references therein. More recently, variance reduction has been used to show linear convergence for smooth and strongly convex finite-sum problems [11]. However, all of these decentralized stochastic algorithms are built on undirected graphs, see [19] for a friendly tutorial. Related work on directed graphs includes [14], [15], [20]–[24] where true gradients are used, and [16], [25]–[27] on stochastic methods, all of which use the push-sum algorithm [28] to achieve agreement with an exception of [15], [27], [29], [30] that employ updates with both row and column stochastic weights to avoid the eigenvector estimation in push-sum.

In this report, we present **S-ADDOPT** for decentralized stochastic optimization over directed graphs. In particular, **S-ADDOPT** adds gradient tracking to **SGP** (stochastic gradient push) [16], [25], [26] and can be viewed as a stochastic extension of **ADDOPT** [14], [31] that uses true gradients. Of significant relevance is [12] that is applicable to undirected graphs and is based on doubly stochastic weights. Since **S-ADDOPT** is based on directed graphs, it essentially extends the algorithm in [12] with the help of push-sum when the network weights are restricted to be column stochastic. A similar algorithm based on row-stochastic weights is also immediate by apply the extension and analysis in this report to FROST [23], [24].

The main contributions of this report are as follows: (i) We develop a stochastic algorithm over directed graphs by combining push-sum with gradient tracking; (ii) For a constant step-size  $\alpha$ , we show that each node converges linearly inside an error ball around the optimal solution, and further show that the size of the error ball is controlled by  $\alpha$ . (iii) For decaying step-sizes  $\mathcal{O}(1/k)$ , we show that **S-ADDOPT** is asymptotically network-independent and reaches the exact solution sublinearly at  $\mathcal{O}(1/k)$ , while the network agreement error decays at a faster rate of  $\mathcal{O}(1/k^2)$ . (iv) We explicitly quantify the directed nature of graphs using a directivity constant  $\tau$ , which makes this work a generalization of **DSGD**, **SGP**, and the method proposed in [12]. The directivity constant  $\tau$  is 1 for undirected graphs and thus the results apply to undirected graphs as a special case. The rest of this report is organized as follows. We formalize the optimization problem, list the underlying assumptions, and describe **S-ADDOPT** in Section II. We then present the main results in Section III and the convergence analysis in Section IV. Finally, we provide numerical experiments in Section V and conclude the report in Section VI.

**Basic Notation:** We use uppercase italic letters for matrices and lowercase bold letters for vectors. We use  $I_n$  for the  $n \times n$  identity matrix and  $\mathbf{1}_n$  denotes the column vector of  $n$  ones. A column stochastic matrix is such that it is non-negative and all of its columns sum to 1. For a primitive column stochastic matrix  $B \in \mathbb{R}^{n \times n}$ , we have  $B^\infty = \pi \mathbf{1}_n^\top$ , from the Perron-Frobenius theorem [32], where  $\pi$  and  $\mathbf{1}_n^\top$  are its right and left Perron eigenvectors. For a matrix  $G$ ,  $\rho(G)$  is its spectral radius. We denote the Euclidean (vector) norm by  $\|\cdot\|_2$  and define a weighted inner product as  $\langle \mathbf{x}, \mathbf{y} \rangle_\pi := \mathbf{x}^\top \text{diag}(\pi)^{-1} \mathbf{y}$ , for  $\mathbf{x}, \mathbf{y} \in \mathbb{R}^p$ , which leads to a weighted Euclidean norm:  $\|\mathbf{x}\|_\pi := \|\text{diag}(\sqrt{\pi})^{-1} \mathbf{x}\|_2$ . We denote  $\| \cdot \|_\pi$  as the matrix norm induced by  $\|\cdot\|_\pi$  such that  $\forall X \in \mathbb{R}^{n \times n}$ ,  $\|X\| := \|\|\text{diag}(\sqrt{\pi})^{-1} X \text{diag}(\sqrt{\pi})\|_2\|$ . Note that these norms are related as  $\|\cdot\|_\pi \leq \underline{\pi}^{-0.5} \|\cdot\|_2$  and  $\|\cdot\|_2 \leq \bar{\pi}^{0.5} \|\cdot\|_\pi$ , where  $\bar{\pi}$  and  $\underline{\pi}$  are the maximum and minimum elements in  $\pi$ , while  $\|B\|_\pi = \|B^\infty\|_\pi = \|I_n - B^\infty\|_\pi = 1$ . Finally, it is shown in [27] that  $\sigma_B := \|\|B - B^\infty\|_\pi < 1$ .

## II. PROBLEM FORMULATION

Consider  $n$  nodes communicating over a strongly-connected directed graph (digraph),  $\mathcal{G} = (\mathcal{V}, \mathcal{E})$ , where  $\mathcal{V} = \{1, 2, 3, \dots, n\}$  is the set of agents and  $\mathcal{E}$  is the collection of ordered pairs,  $(i, j), i, j \in \mathcal{V}$ , such that node  $i$  receives information from node  $j$ . We let  $\mathcal{N}_i^{\text{out}}$  (resp.  $\mathcal{N}_i^{\text{in}}$ ) to denote the set of out-neighbors (resp. in-neighbors) of node  $i$ , i.e., nodes that can receive information from  $i$ , and  $|\mathcal{N}_i^{\text{out}}|$  is the out-degree of node  $i$ . Note that both  $\mathcal{N}_i^{\text{out}}$  and  $\mathcal{N}_i^{\text{in}}$  include node  $i$ . The nodes collaborate to solve the following optimization problem:

$$\mathbf{P} : \quad \min_{\mathbf{z} \in \mathbb{R}^p} F(\mathbf{z}) := \frac{1}{n} \sum_{i=1}^n f_i(\mathbf{z}),$$

where each node  $i$  possesses a private cost function  $f_i : \mathbb{R}^p \rightarrow \mathbb{R}$ . We make the following assumptions.

**Assumption 1.** *The communication graph  $\mathcal{G}$  is a strongly-connected directed graph and each node has the knowledge of its out-degree  $|\mathcal{N}_i^{\text{out}}|$ .*

**Assumption 2.** *Each local cost function  $f_i$  (and thus  $F$ ) is  $\mu$ -strongly convex and  $\ell$ -smooth, i.e.,  $\forall \mathbf{x}, \mathbf{y} \in \mathbb{R}^p$  and  $\forall i \in \mathcal{V}$ , there exist positive constants  $\mu$  and  $\ell$  such that*

$$\frac{\mu}{2} \|\mathbf{x} - \mathbf{y}\|_2^2 \leq f_i(\mathbf{y}) - f_i(\mathbf{x}) - \nabla f_i(\mathbf{x})^\top (\mathbf{y} - \mathbf{x}) \leq \frac{\ell}{2} \|\mathbf{x} - \mathbf{y}\|_2^2.$$

Note that the ratio  $\kappa := \frac{\ell}{\mu}$  is called the condition number of the function  $f_i$ . We have that  $\ell \geq \mu$  and thus  $\kappa \geq 1$ .

**Assumption 3.** *Each node has access to a stochastic first-order oracle SFO that returns a stochastic gradient  $\nabla \widehat{f}_i(\mathbf{z}_k^i)$  for any  $\mathbf{z}_k^i \in \mathbb{R}^p$  such that*

$$\begin{aligned} \mathbb{E} \left[ \nabla \widehat{f}_i(\mathbf{z}_k^i) | \mathbf{z}_k^i \right] &= \nabla f_i(\mathbf{z}_k^i), \\ \mathbb{E} \left[ \|\nabla \widehat{f}_i(\mathbf{z}_k^i) - \nabla f_i(\mathbf{z}_k^i)\|_2^2 | \mathbf{z}_k^i \right] &\leq \sigma^2. \end{aligned}$$

These assumptions are standard in the related literature. The bounded variance assumption however can be relaxed, see [6], for example. Due to Assumption 2, we note that  $F$  has a unique minimizer that is denoted by  $\mathbf{z}^*$ . The proposed algorithm to solve Problem  $\mathbf{P}$  is described next.

### A. **S-ADDOPT**: Algorithm

The **S-ADDOPT** algorithm to solve Problem  $\mathbf{P}$  is formally described in Algorithm 1. We note that the set of weights  $\underline{B} = \{b_{ij}\}$  is such that  $\underline{B}$  is column stochastic. A valid choice is  $b_{ji} = |\mathcal{N}_i^{\text{out}}|^{-1}$ , for each  $j \in \mathcal{N}_i^{\text{out}}$  and zero otherwise, recall Assumption 1. Each agent  $i$  maintains three state vectors, i.e.,  $\mathbf{x}_k^i, \mathbf{w}_k^i, \mathbf{z}_k^i \in \mathbb{R}^p$  and a (positive) scalar  $y_k^i$  at each iteration  $k$ . The first update  $\mathbf{x}_{k+1}^i$  is similar to **DSGD**, where the stochastic gradient  $\nabla \widehat{f}_i(\mathbf{x}_k^i)$  is replaced with  $\mathbf{w}_k^i$ . This auxiliary variable  $\mathbf{w}_k^i$  is based on dynamic average-consensus [33] and in fact tracks the global gradient  $\nabla F$  when viewed as a non-stochastic update (see [13]–[15], [34] for details). However, since the weight matrix  $\underline{B}$  is not row-stochastic, the variables  $\mathbf{x}_k^i$ 's do not agree on a solution and converge with a certain imbalance that is due to the fact that  $\mathbf{1}_n$  is not the right Perron eigenvector of  $\underline{B}$ . This imbalance is canceled in

the  $\mathbf{z}_k^i$ -update with the help of a scaling by  $y_k^i$ , since  $y_k^i$  estimates the  $i$ -th component of  $\boldsymbol{\pi}$  (recall that  $\underline{B}\boldsymbol{\pi} = \boldsymbol{\pi}$ ). We note that **S-ADDOPT** is in fact a stochastic extension of **ADDOPT**, where true local gradients  $\nabla f_i$ 's are used at each node.

---

**Algorithm 1 S-ADDOPT:** At each node  $i$

---

**Require:**  $\mathbf{x}_0^i \in \mathbb{R}^p, \mathbf{z}_0^i = \mathbf{x}_0^i, y_0^i = 1, \mathbf{w}_0^i = \nabla \widehat{f}_i(\mathbf{z}_0^i), \alpha > 0$

1: **for**  $k = 0, 1, 2, \dots$  **do**

2:   **State update:**  $\mathbf{x}_{k+1}^i = \sum_{j=1}^n b_{ij} \mathbf{x}_k^j - \alpha \mathbf{w}_k^i$

3:   **Eigenvector est.:**  $y_{k+1}^i = \sum_{j=1}^n b_{ij} y_k^j$

4:   **Push-sum update:**  $\mathbf{z}_{k+1}^i = \mathbf{x}_{k+1}^i / y_{k+1}^i$

5:   **Gradient tracking update:**  $\mathbf{w}_{k+1}^i = \sum_{j=1}^n b_{ij} \mathbf{w}_k^j + \nabla \widehat{f}_i(\mathbf{z}_{k+1}^i) - \nabla \widehat{f}_i(\mathbf{z}_k^i)$

6: **end for**

---

**S-ADDOPT** can be compactly written in a vector form with the help of the following notation. Let  $\mathbf{x}_k, \mathbf{z}_k, \mathbf{w}_k$ , all in  $\mathbb{R}^{np}$  concatenate the local states  $\mathbf{x}_k^i, \mathbf{z}_k^i, \mathbf{w}_k^i$  (all in  $\mathbb{R}^p$ ) at the nodes and  $\mathbf{y}_k \in \mathbb{R}^n$  stacks the  $y_k^i$ 's. Let  $\otimes$  denote the Kronecker product and define  $B := \underline{B} \otimes I_p$ , and let  $Y_k := \text{diag}(\mathbf{y}_k) \otimes I_p$ . Then **S-ADDOPT** described in Algorithm 1 can be written in a vector form as

$$\mathbf{x}_{k+1} = B\mathbf{x}_k - \alpha \mathbf{w}_k, \quad (1a)$$

$$\mathbf{y}_{k+1} = \underline{B}\mathbf{y}_k, \quad (1b)$$

$$\mathbf{z}_{k+1} = Y_{k+1}^{-1} \mathbf{x}_{k+1}, \quad (1c)$$

$$\mathbf{w}_{k+1} = B\mathbf{w}_k + \nabla \widehat{f}(\mathbf{z}_{k+1}) - \nabla \widehat{f}(\mathbf{z}_k). \quad (1d)$$

In the following sections, we summarize the main results (Section III) and provide the convergence analysis (Section IV) of **S-ADDOPT**. Subsequently, we compare its performance with related algorithms on digraphs in Section V.

### III. MAIN RESULTS

We use  $p = 1$  for simplicity and thus  $B = \underline{B}$ . Before we proceed, we define  $\bar{\mathbf{x}}_k := \frac{1}{n} \mathbf{1}_n^\top \mathbf{x}_k$ , and  $\widehat{\mathbf{x}}_k := B^\infty \mathbf{x}_k$ , which are the mean and weighted averages of  $\mathbf{x}_k^i$ 's, respectively, and  $y := \sup_k \|Y_k\|_2$ ,  $y_- := \sup_k \|Y_k^{-1}\|_2$ . We next provide two useful lemmas.

**Lemma 1.** [14], [27] Consider Assumption 1 and define  $Y^\infty := \lim_{k \rightarrow \infty} Y_k$ ,  $h := \bar{\pi}/\underline{\pi}$ , and  $\beta := \sqrt{h} \|\mathbf{1}_n - n\boldsymbol{\pi}\|_2$ . Then  $\|Y_k - Y^\infty\|_2 \leq \beta \sigma_B^k, \forall k \geq 0$ .

*Proof.* Note that  $\forall k \geq 0, \mathbf{y}_\infty = B^\infty \mathbf{y}_k$ . Thus we have

$$\|Y_k - Y^\infty\|_2 \leq \|\mathbf{y}_k - \mathbf{y}_\infty\|_2 \leq \sqrt{\bar{\pi}} \|B - B^\infty\|_\pi \|\mathbf{y}_{k-1} - \mathbf{y}_\infty\|_\pi \leq \sigma_B^k \sqrt{h} \|\mathbf{y}_0 - \mathbf{y}_\infty\|_2.$$

and the proof follows.  $\square$

**Lemma 2.** Define  $\mathbf{e}_k := \frac{1}{n} \mathbb{E}[\|\mathbf{z}_k - \mathbf{1}_n \mathbf{z}^*\|_2^2]$  as the mean error in the network. We have

$$\mathbf{e}_k \leq \frac{\omega}{n} \mathbb{E}\|\mathbf{x}_k - \widehat{\mathbf{x}}_k\|_{\pi}^2 + \omega \beta^2 \sigma_B^k \|\mathbf{z}^*\|_2^2 + \omega y^2 \mathbb{E}\|\bar{\mathbf{x}}_k - \mathbf{z}^*\|_{\pi}^2, \quad (2)$$

$$\mathbf{e}_k \leq \psi \mathbb{E}\|\mathbf{x}_k - \widehat{\mathbf{x}}_k\|_{\pi}^2 + \psi \beta \sigma_B^k \mathbb{E}\|\mathbf{x}_k\|_{\pi}^2 + 2\mathbb{E}\|\bar{\mathbf{x}}_k - \mathbf{z}^*\|_2^2, \quad (3)$$

where  $\omega := 3y_-^2 \bar{\pi}$  and  $\psi := 2y_-^2 \bar{\pi}(1 + \beta)/n$ .

We now provide the main results on **S-ADDOPT**.

**Theorem 1.** Let Assumptions 1, 2, and 3 hold and let the step-size  $\alpha$  be a constant such that,

$$\alpha \leq \frac{1}{\ell \sqrt{\kappa}} \cdot \frac{(1 - \sigma_B^2)^2}{51 \sqrt{\tau}}, \quad (4)$$

where  $\tau := y_-^6 y^2 h(1 + \beta)$  is the directivity constant. Then  $\mathbf{e}_k$  converges linearly, at a rate  $\gamma, \gamma \in [0, 1)$ , to a ball around  $\mathbf{z}^*$ , i.e.,

$$\limsup_{k \rightarrow \infty} \mathbf{e}_k = \alpha \mathcal{O}\left(\frac{\sigma^2}{n\mu}\right) + \alpha^2 \mathcal{O}\left(\frac{\ell^2 \sigma^2}{\mu^2 (1 - \sigma_B^2)^4}\right). \quad (5)$$

The proof of Theorem 1 is provided in the next Section. It essentially shows that **S-ADDOPT** converges linearly with a constant step-size to an error ball around  $\mathbf{z}^*$ , the size of which however is controlled by  $\alpha$ . We note that  $\tau \geq 1$  can be considered as a directivity constant and is large when the graph is more directed as quantified by e.g., the constant  $h$  (in addition to the other constants in  $\tau$ ); clearly, for undirected graphs  $\tau = 1$  and thus Theorem 1 is applicable to undirected graphs as a special case. We further note that the first term in (5) is due to the variance  $\sigma^2$  of the stochastic gradients and does not have a network dependence, i.e., a scaling with  $(1 - \sigma_B^2)^{-1}$ . The rate of convergence of **S-ADDOPT** thus is comparable to the **SGD** (up to some constant factors) when the step-size  $\alpha$  is sufficiently small since the second term has a higher order of  $\alpha$ . The result in Theorem 1 is similar to what was obtained for undirected graphs in [12], where the network dependence is  $\mathcal{O}((1 - \sigma_B^2)^{-3})$ . We next provide an upper bound on the linear rate  $\gamma$ .

**Corollary 1.** Let Assumptions 1, 2 and 3 hold. If the step-size follows  $\alpha \leq \frac{3}{40} \left(\frac{1 - \sigma_B^2}{\mu}\right)$ , then the linear rate parameter  $\gamma$  in Theorem 1 is such that

$$\gamma \leq 1 - \frac{\alpha \mu}{3}.$$

The proof of Corollary 1 is available in Appendix B and follows the same arguments as in [12]. Going back to Theorem 1, note that the exact expression of (5) is provided later in the convergence analysis, see (15), where we dropped the higher powers of  $\alpha$  when writing (5). We note from (15) that all terms in the residual are a function of  $\sigma^2$  and thus **S-ADDOPT** recovers the exact linear convergence as  $\sigma^2$  vanishes. When  $\sigma^2$  is not zero, exact convergence is achievable albeit at a sublinear rate with decaying step-sizes. We provide this result below.

**Theorem 2.** Let Assumptions 1, 2, and 3 hold. Consider **S-ADDOPT** with decaying step-sizes  $\alpha_k := \frac{\theta}{m+k}, \theta > \frac{1}{\mu}$  and  $m$  such that

$$\left\{ \begin{array}{l} m > \max \left\{ \frac{\theta(\ell+\mu)}{2}, \frac{6\ell\theta y_- \sqrt{(1+\sigma_B^2)h}}{1-\sigma_B^2} \right\}, \\ \frac{(1-\sigma_B^2)^2}{6\theta^2(1+\sigma_B^2)} \left( \frac{1-\sigma_B^2}{2} - \frac{2m+1}{(m+1)^2} \right) > \frac{E_2}{m^2} + \left( \frac{\theta^3 \ell^6 E_1 E_3}{m^4 n (\theta\mu-1)} \right) \left( \frac{\theta\mu+m}{m\mu} \right), \end{array} \right.$$

for some constants  $E_1, E_2, E_3$ . Select  $\tilde{S}$  large enough such that  $\forall k \geq \tilde{S}, \sigma_B^k \leq \frac{1}{n(m+k)^2}$ , then we have

$$\begin{aligned} \mathbb{E} \|\mathbf{x}_k - \hat{\mathbf{x}}_k\|_{\pi}^2 &\leq \frac{\mathcal{O}(1)}{(m+k)^2}, \\ \mathbb{E} \|\bar{\mathbf{x}}_k - \mathbf{z}^*\|_2^2 &\leq \frac{2\theta^2\sigma^2}{n(\theta\mu-1)(m+k)} + \frac{\mathcal{O}(1)}{(m+k)\theta\mu} + \frac{\mathcal{O}(1)}{(m+k)^2}, \end{aligned}$$

which leads to  $\mathbf{e}_k \rightarrow 0$  at a network-independent convergence rate of  $\mathcal{O}(\frac{1}{k})$ .

Theorem 2, formally analyzed in the next section, shows that the error  $\mathbf{e}_k$  in **S-ADDOPT** asymptotically converges to the exact solution at a rate dominant by  $\frac{4\theta^2\sigma^2}{n(\theta\mu-1)k}$ , which is network-independent since all other terms decay faster, and thus **S-ADDOPT** matches the rate of **SGD** (up to some constant factors); see also [12], [16]–[18]. It can also be verified that the network reaches an agreement at  $\mathcal{O}(1/k^2)$ .

#### IV. CONVERGENCE ANALYSIS

To aid the analysis of Theorems 1 and 2, we first develop a dynamical system that characterizes **S-ADDOPT** for both constant and decaying step-sizes. We find inter-relationships between the following three terms:

- (i) Network agreement error,  $\mathbb{E} \|\mathbf{x}_k - B^\infty \mathbf{x}_k\|_{\pi}^2$ ,
- (ii) Optimality gap,  $\mathbb{E} \|\bar{\mathbf{x}}_k - \mathbf{z}^*\|_2^2$ ,
- (iii) Gradient tracking error,  $\mathbb{E} \|\mathbf{w}_k - B^\infty \mathbf{w}_k\|_{\pi}^2$ ,

to write an LTI system of equations governing **S-ADDOPT**. For simplicity, we assume  $p = 1$ . Denote  $\mathbf{t}_k, \mathbf{s}_k, \mathbf{c} \in \mathbb{R}^3$ , and  $A_\alpha, H_k \in \mathbb{R}^{3 \times 3}$  for all  $k$  as

$$\begin{aligned} \mathbf{t}_k &:= \begin{bmatrix} \mathbb{E} [\|\mathbf{x}_k - B^\infty \mathbf{x}_k\|_{\pi}^2] \\ \mathbb{E} [\|\bar{\mathbf{x}}_k - \mathbf{z}^*\|_2^2] \\ \mathbb{E} [\|\mathbf{w}_k - B^\infty \mathbf{w}_k\|_{\pi}^2] \end{bmatrix}, \quad \mathbf{s}_k := \begin{bmatrix} \mathbb{E} [\|\mathbf{x}_k\|_2^2] \\ 0 \\ 0 \end{bmatrix}, \quad \mathbf{c} := \begin{bmatrix} 0 \\ \alpha^2 \frac{\sigma^2}{n} \\ C_\sigma \end{bmatrix}, \\ H_k &:= \begin{bmatrix} 0 & 0 & 0 \\ h_1 \sigma_B^k & 0 & 0 \\ (h_2 + \alpha^2 h_3) \sigma_B^k & 0 & 0 \end{bmatrix}, \quad A_\alpha := \begin{bmatrix} \frac{1+\sigma_B^2}{2} & 0 & \alpha^2 \frac{1+\sigma_B^2}{1-\sigma_B^2} \\ \alpha^2 g_1 + \alpha g_2 & 1 - \alpha\mu & 0 \\ g_3 + \alpha^2 g_4 & \alpha^2 g_5 & \frac{5+\sigma_B^2}{6} \end{bmatrix}, \end{aligned} \quad (6)$$

where the constants are defined as:

$$\begin{aligned} g_1 &:= \left( \frac{\ell^2 y_-^2}{n} \right) (1 + \beta \sigma_B) \bar{\pi}, & g_2 &:= \left( \frac{\ell^2 y_-^2}{n\mu} \right) (1 + \beta \sigma_B) \bar{\pi}, & g_3 &:= 4k_2, \\ g_4 &:= 2\ell^2 y_-^2 k_2 k_3 (1 + \beta \sigma_B), & g_5 &:= 18\ell^4 q y_-^4 y^2 \bar{\pi}^{-1}, & k_1 &:= \frac{1-\sigma_B^2}{3}, \\ C_\sigma &:= \sigma^2 (c_1 + \alpha^2 c_2), & c_1 &:= 4qn \bar{\pi}^{-1}, & k_2 &:= 6\ell^2 q y_-^2 h \\ c_2 &:= 12\ell^2 q y_-^4 y^2 k_3 \bar{\pi}^{-1}, & h_1 &:= y_-^2 \beta \left( \frac{\alpha \ell^2}{\mu} + \alpha^2 \ell^2 \right) (\beta + 1), & k_3 &:= \frac{2k_1 - 3k_2 \alpha^2}{k_1 - 2k_2 \alpha^2}, \\ h_2 &:= 24\ell^2 q y_-^4 \beta^2 \bar{\pi}^{-1}, & h_3 &:= 12\ell^4 q y_-^6 y^2 k_3 \beta \bar{\pi}^{-1} (\beta + 1), & q &:= \frac{1+\sigma_B^2}{1-\sigma_B^2}. \end{aligned}$$

With  $\alpha \leq \left(\frac{1-\sigma_B^2}{9\ell}\right) \frac{1}{y-\sqrt{h}}$ , we have that

$$\mathbf{t}_{k+1} \leq A_\alpha \mathbf{t}_k + H_k \mathbf{s}_k + \mathbf{c}. \quad (7)$$

The derivation of the above inequality is available in Appendix A. We now provide the proofs of Theorems 1 and 2.

### A. Proof of Theorem 1

From [12] Lemma 5, for a  $3 \times 3$  non-negative, irreducible matrix  $A_\alpha = \{a_{ij}\}$  with  $\{a_{ii}\} < \lambda^*$ , we have  $\rho(A_\alpha) < \lambda^*$  if and only if  $\det(\lambda^* I_3 - A_\alpha) > 0$ . For  $A_\alpha$  in (6),  $a_{11}, a_{33} < 1$  since  $\sigma_B \in [0, 1)$ , and  $a_{22} < 1$  since  $\alpha < \frac{1}{\ell}$  and  $\ell \geq \mu$ . Expanding the determinant as

$$\begin{aligned} \det(I_3 - A_\alpha) &= (1 - a_{11})(1 - a_{22})(1 - a_{33}) - a_{13}[a_{21}a_{32} + (1 - a_{22})a_{31}] \\ &= (1 - a_{22}) \left[ (1 - a_{11})(1 - a_{33}) - a_{13}a_{31} \right] - a_{13}a_{21}a_{32}, \end{aligned}$$

we note that if the following is true for some  $\Gamma > 1$ ,

$$-a_{13}a_{31} \geq -\frac{1}{\Gamma}(1 - a_{11})(1 - a_{33}), \quad (8)$$

$$-a_{13}a_{21}a_{32} \geq -\frac{\Gamma - 1}{\Gamma(\Gamma + 1)}(1 - a_{11})(1 - a_{22})(1 - a_{33}), \quad (9)$$

then we obtain

$$\begin{aligned} \det(I_3 - A_\alpha) &\geq (1 - a_{22}) \left[ (1 - a_{11})(1 - a_{33}) - \frac{1}{\Gamma}(1 - a_{11})(1 - a_{33}) \right] - \frac{\Gamma - 1}{\Gamma(\Gamma + 1)}(1 - a_{11})(1 - a_{22})(1 - a_{33}) \\ &\geq (1 - a_{22})(1 - a_{11})(1 - a_{33}) \frac{\Gamma - 1}{\Gamma} - \frac{\Gamma - 1}{\Gamma(\Gamma + 1)}(1 - a_{11})(1 - a_{22})(1 - a_{33}) \\ &\geq \left( \frac{\Gamma - 1}{\Gamma + 1} \right) (1 - a_{22})(1 - a_{11})(1 - a_{33}) > 0, \end{aligned}$$

ensuring  $\rho(A_\alpha) < 1$ . We thus find the range of  $\alpha$  that satisfies (8) and (9). Using  $\{a_{ij}\}$ 's from (6) in (8), we get

$$\begin{aligned} \alpha^2 q (g_3 + \alpha^2 g_4) &\leq \frac{1}{\Gamma} \left( \frac{1 - \sigma_B^2}{2} \right) \left( \frac{1 - \sigma_B^2}{6} \right) \\ \alpha^2 k_2 (4 + \alpha^2 2\ell^2 y^2 \frac{2k_1 - 3k_2 \alpha^2}{k_1 - 2k_2 \alpha^2} (1 + \beta \sigma_B)) &\leq \frac{1}{12\Gamma} \left( \frac{(1 - \sigma_B^2)^3}{1 + \sigma_B^2} \right) \\ \alpha^2 k_2 \left( \frac{4k_1 - 8k_2 \alpha^2 + 2\alpha^2 \ell^2 y^2 (1 + \beta \sigma_B) (2k_1 - 3k_2 \alpha^2)}{k_1 - 2k_2 \alpha^2} \right) &\leq \frac{1}{12\Gamma} \left( \frac{(1 - \sigma_B^2)^3}{1 + \sigma_B^2} \right) \\ \alpha^2 k_2 (4k_1 + 4k_1 \alpha^2 \ell^2 y^2 (1 + \beta \sigma_B)) + \frac{2k_2 \alpha^2}{12\Gamma} \left( \frac{(1 - \sigma_B^2)^3}{1 + \sigma_B^2} \right) &\leq \frac{1}{36\Gamma} \left( \frac{(1 - \sigma_B^2)^4}{1 + \sigma_B^2} \right) + 8k_2^2 \alpha^4 + 6k_2^2 \alpha^6 \ell^2 y^2 (1 + \beta \sigma_B) \\ \alpha^2 k_2 \left( 4k_1 + 4k_1 \ell^2 y^2 (1 + \beta \sigma_B) \alpha^2 + \frac{2}{12\Gamma} \left( \frac{(1 - \sigma_B^2)^3}{1 + \sigma_B^2} \right) \right) &\leq \frac{1}{36\Gamma} \left( \frac{(1 - \sigma_B^2)^4}{1 + \sigma_B^2} \right) + 8k_2^2 \alpha^4 \\ &\quad + 6k_2^2 \ell^2 y^2 (1 + \beta \sigma_B) \alpha^6 \\ \alpha^2 k_1 k_2 \left( 4 + 4\ell^2 y^2 (1 + \beta \sigma_B) \alpha^2 + \frac{1}{2\Gamma} \left( \frac{(1 - \sigma_B^2)^2}{1 + \sigma_B^2} \right) \right) &\leq \frac{1}{36\Gamma} \left( \frac{(1 - \sigma_B^2)^4}{1 + \sigma_B^2} \right) + 8k_2^2 \alpha^4 \\ &\quad + 6k_2^2 \ell^2 y^2 (1 + \beta \sigma_B) \alpha^6. \end{aligned}$$

We now simplify the above condition by letting  $\alpha \leq \left(\frac{1-\sigma_B^2}{9\ell y_-}\right) \sqrt{\frac{\pi}{\pi}}$  in the LHS and decreasing the RHS, which leads to

$$\begin{aligned}
\alpha^2 &\leq \frac{\frac{1}{36\Gamma} \frac{(1-\sigma_B^2)^4}{1+\sigma_B^2}}{(2\ell^2 y_-^2 \pi^{-1} \bar{\pi} (1+\sigma_B^2)) \left(4 + 4 \left(\frac{(1-\sigma_B^2)\sqrt{\pi}}{9y_- \sqrt{\pi}}\right)^2 y^2 (1+\beta\sigma_B) + \frac{1}{2\Gamma} \left(\frac{(1-\sigma_B^2)^2}{1+\sigma_B^2}\right)\right)} \\
&= \frac{\frac{(1-\sigma_B^2)^4}{1+\sigma_B^2}}{(\ell^2 y_-^2 \pi^{-1} \bar{\pi} (1+\sigma_B^2)) \left(288\Gamma + 288\Gamma \left(\frac{(1-\sigma_B^2)\sqrt{\pi}}{9y_- \sqrt{\pi}}\right)^2 y^2 (1+\beta\sigma_B) + 36\frac{(1-\sigma_B^2)^2}{1+\sigma_B^2}\right)} \\
\Leftarrow \alpha^2 &\leq \frac{y_-^2 \frac{(1-\sigma_B^2)^4}{1+\sigma_B^2}}{\ell^2 y_-^2 h(1+\sigma_B^2) \left(288y_-^2 \Gamma + 4\Gamma(1-\sigma_B^2)^2 h^{-1} y^2 (1+\beta\sigma_B) + 36y_-^2 \frac{(1-\sigma_B^2)^2}{1+\sigma_B^2}\right)} \\
&= \frac{y_-^2 (1-\sigma_B^2)^4}{\ell^2 y_-^2 h(1+\sigma_B^2) (288y_-^2 \Gamma(1+\sigma_B^2) + 4\Gamma(1-\sigma_B^2)^2 h^{-1} y^2 (1+\beta\sigma_B)(1+\sigma_B^2) + 36y_-^2 (1-\sigma_B^2)^2)}.
\end{aligned}$$

We use  $\sigma_B < 1$ ,  $(1-\sigma_B^2) < 1$ ,  $(1+\sigma_B^2) < 2$ ,  $y^2(1+\beta) \geq 1$ ,  $hy_-^2 \geq 1$  and  $\Gamma hy^2(1+\beta) > 1$  leading to

$$\alpha^2 \leq \frac{y_-^2 (1-\sigma_B^2)^4}{2\ell^2 y_-^2 (612\Gamma hy_-^2 y^2 (1+\beta) + 8\Gamma hy_-^2 y^2 (1+\beta))} = \frac{(1-\sigma_B^2)^4}{1240\ell^2 (\Gamma hy_-^2 y^2 (1+\beta))}.$$

Taking square root of both sides results into

$$\alpha \leq \frac{(1-\sigma_B^2)^2}{36\ell y_- y \sqrt{\Gamma h(1+\beta)}}.$$

We next note that (9) holds when

$$\begin{aligned}
(\alpha^2 q)(\alpha^2 g_1 + \alpha g_2)(\alpha^2 g_5) &\leq \frac{\Gamma-1}{\Gamma(\Gamma+1)} \left(1 - \left(\frac{1+\sigma_B^2}{2}\right)\right) (1 - (1-\alpha\mu)) \left(1 - \frac{5+\sigma_B^2}{6}\right) \\
\alpha^5 q g_5 (\alpha g_1 + g_2) &\leq \frac{\Gamma-1}{\Gamma(\Gamma+1)} \left(\frac{1-\sigma_B^2}{2}\right) (\alpha\mu) \left(\frac{1-\sigma_B^2}{6}\right) \\
\alpha^4 q g_5 g_2 (1+\alpha\mu) &\leq \frac{\Gamma-1}{\Gamma(\Gamma+1)} \left(\frac{1-\sigma_B^2}{2}\right)^2 \left(\frac{\mu}{3}\right),
\end{aligned}$$

which can be simplified by using  $\alpha \leq \frac{1}{\mu}$ , i.e.,

$$\begin{aligned}
\alpha^4 &\leq \frac{\Gamma-1}{\Gamma(\Gamma+1)} \left(\frac{(1-\sigma_B^2)^3}{1+\sigma_B^2}\right) \left(\frac{\mu}{24}\right) \left(\frac{\mu}{\ell^6 (18y_-^6 y^2 \pi^{-1} \bar{\pi}) (1+\beta\sigma_B)}\right) \\
\Leftarrow \alpha^4 &\leq \frac{\Gamma-1}{\Gamma(\Gamma+1)} \left(\frac{(1-\sigma_B^2)^3 \mu^2}{864\ell^6 (y_-^6 y^2 \pi^{-1} \bar{\pi}) (1+\beta\sigma_B)}\right) \\
\Leftarrow \alpha &\leq \frac{1}{6\ell\sqrt{\kappa}} \left[\frac{\Gamma-1}{\Gamma(\Gamma+1)} \left(\frac{(1-\sigma_B^2)^3}{y_-^6 y^2 h(1+\beta\sigma_B)}\right)\right]^{\frac{1}{4}},
\end{aligned}$$

for which it is sufficient to have

$$\alpha \leq \frac{(1-\sigma_B^2)^{3/4}}{12\ell\sqrt{\kappa}} \left(\frac{\Gamma-1}{\Gamma^2 y_-^6 y^2 h(1+\beta)}\right)^{\frac{1}{4}}. \tag{10}$$

We next select the minimum of all the bounds on step-size,

$$\begin{aligned} \alpha &\leq \min \left\{ \frac{1 - \sigma_B^2}{9\ell y_- \sqrt{h}}, \frac{(1 - \sigma_B^2)^2}{36\ell y_- y \sqrt{\Gamma h(1 + \beta)}}, \frac{(1 - \sigma_B^2)^{3/4}}{12\ell \sqrt{\kappa}} \left( \frac{\Gamma - 1}{\Gamma^2 y_-^6 y^2 h(1 + \beta)} \right)^{\frac{1}{4}} \right\} \\ \Leftrightarrow \alpha &\leq \frac{(1 - \sigma_B^2)^2}{36\ell \sqrt{\kappa}} \cdot \min \left\{ \left( \frac{1}{\tau \Gamma} \right)^{\frac{1}{2}}, \left( \frac{\Gamma - 1}{\tau \Gamma^2} \right)^{\frac{1}{4}} \right\} \\ \Leftrightarrow \alpha &\leq \frac{(1 - \sigma_B^2)^2}{36\ell \sqrt{\kappa}} \cdot \frac{1}{\sqrt{\tau \Gamma}} \cdot \min \left\{ 1, (\Gamma - 1)^{\frac{1}{4}} \right\}, \end{aligned}$$

where  $\tau := y_-^6 y^2 h(1 + \beta)$ . We note that the above is true for all  $\Gamma > 1$  and  $\min \left\{ 1, (\Gamma - 1)^{\frac{1}{4}} \right\}$  is maximized at  $\Gamma = 2$ . Hence, for a largest possible  $\alpha$ , that is feasible given our bound, we select  $\Gamma = 2$ , which leads to

$$\alpha \leq \frac{1}{\ell \sqrt{\kappa}} \cdot \frac{(1 - \sigma_B^2)^2}{51 \sqrt{\tau}}.$$

Thus, when  $\alpha$  follows the above relation, we have  $\rho(A_\alpha) < 1$  and using the linear system recursion in (7), we get

$$\lim_{k \rightarrow \infty} \mathbf{t}_{k+1} \leq (I_3 - A_\alpha)^{-1} \mathbf{c}, \quad (11)$$

since  $\lim_{k \rightarrow \infty} H_k$  is a zero matrix. The first two elements in the R.H.S (vector) of (11) can be manipulated as follows:

$$\begin{aligned} [(I_3 - A_\alpha)^{-1} \mathbf{c}]_1 &= \frac{a_{13} a_{32} \frac{\alpha^2 \sigma^2}{n} + a_{13} (1 - a_{22}) C_\sigma}{\det(I_3 - A_\alpha)} \\ &\leq \left( \frac{\Gamma + 1}{\Gamma - 1} \right) \frac{a_{13}}{(1 - a_{11})(1 - a_{22})(1 - a_{33})} \left[ a_{32} \frac{\alpha^2 \sigma^2}{n} + (1 - a_{22}) C_\sigma \right] \\ &\leq \left( \frac{\alpha^2 \left( \frac{1 + \sigma_B^2}{1 - \sigma_B^2} \right)}{\left( \frac{1 - \sigma_B^2}{2} \right) (\alpha \mu) \left( \frac{1 - \sigma_B^2}{6} \right)} \right) \left[ \alpha^2 (18\ell^4 y_-^4 y^2 \pi^{-1}) \left( \frac{1 + \sigma_B^2}{1 - \sigma_B^2} \right) \left( \frac{\alpha^2 \sigma^2}{n} \right) + (\alpha \mu) C_\sigma \right] \\ &\leq \left( \frac{12\alpha (1 + \sigma_B^2)}{\mu (1 - \sigma_B^2)^3} \right) \left[ 18\alpha^4 \ell^4 y_-^4 y^2 \pi^{-1} \left( \frac{1 + \sigma_B^2}{1 - \sigma_B^2} \right) \left( \frac{\sigma^2}{n} \right) + \alpha \mu (4\sigma^2 n \pi^{-1}) \left( \frac{1 + \sigma_B^2}{1 - \sigma_B^2} \right) \right] \\ &= \alpha^5 \left( \frac{\ell^4 \sigma^2}{n \mu} \right) \left( \frac{216 y_-^4 y^2 \pi^{-1} (1 + \sigma_B^2)^2}{(1 - \sigma_B^2)^4} \right) + \alpha^2 (n \sigma^2) \left( \frac{48 \pi^{-1} (1 + \sigma_B^2)^2}{(1 - \sigma_B^2)^4} \right) \\ &= \frac{\alpha^5}{(1 - \sigma_B^2)^4} \mathcal{O} \left( \frac{\ell^4 \sigma^2}{n \mu} \right) + \frac{\alpha^2}{(1 - \sigma_B^2)^4} \mathcal{O} (n \sigma^2); \end{aligned} \quad (12)$$

$$\begin{aligned} [(I_3 - A_\alpha)^{-1} \mathbf{c}]_2 &= \frac{[(1 - a_{11})(1 - a_{33}) - a_{13} a_{31}] \frac{\alpha^2 \sigma^2}{n} + (a_{13} a_{21}) C_\sigma}{\det(I_3 - A_\alpha)} \\ &\leq \frac{\Gamma + 1}{\Gamma} \left( \frac{\alpha^2 \sigma^2}{n(1 - a_{22})} \right) + \left( \frac{\Gamma + 1}{\Gamma - 1} \right) \left( \frac{a_{13} a_{21} C_\sigma}{(1 - a_{11})(1 - a_{22})(1 - a_{33})} \right) \\ &\leq \frac{\alpha^2 \sigma^2}{n(\alpha \mu)} + \frac{\alpha^2 \left( \frac{1 + \sigma_B^2}{1 - \sigma_B^2} \right) \left( \alpha^2 \left( \frac{\ell^2 y_-^2 (1 + \beta \sigma_B) \bar{\pi}}{n} \right) + \alpha \left( \frac{\ell^2 y_-^2 (1 + \beta \sigma_B) \bar{\pi}}{n \mu} \right) \right) C_\sigma}{\left( \frac{1 - \sigma_B^2}{2} \right) (\alpha \mu) \left( \frac{1 - \sigma_B^2}{6} \right)} \\ &= \frac{\alpha \sigma^2}{n \mu} + \frac{12\alpha (1 + \sigma_B^2)^2 \left( \alpha^2 (\ell^2 y_-^2 (1 + \beta \sigma_B) \bar{\pi}) + \alpha \left( \frac{\ell^2 y_-^2 (1 + \beta \sigma_B) \bar{\pi}}{\mu} \right) \right) (4\sigma^2 n \pi^{-1})}{n \mu (1 - \sigma_B^2)^4} \\ &= \alpha \mathcal{O} \left( \frac{\sigma^2}{n \mu} \right) + \frac{\alpha^2}{(1 - \sigma_B^2)^4} \mathcal{O} \left( \frac{\ell^2 \sigma^2}{\mu^2} \right). \end{aligned} \quad (13)$$

Finally, the mean network error, defined as  $\mathbf{e}_k := \frac{1}{n} \mathbb{E} [\|\mathbf{z}_k - \mathbf{1}_n \mathbf{z}^*\|_2^2]$ , is given by

$$\mathbf{e}_k \leq \frac{3y_-^2 \bar{\pi}}{n} \mathbb{E} [\|\mathbf{x}_k - B^\infty \mathbf{x}_k\|_\pi^2] + 3y_-^2 \beta^2 \mathbb{E} [\|\mathbf{z}^*\|_2^2] \sigma_B^{2k} + 3y_-^2 y^2 \mathbb{E} [\|\mathbf{x}_k - \mathbf{1}_n \mathbf{z}^*\|_2^2]. \quad (14)$$

Notice that the second term of (14) vanishes asymptotically. Using (12) and (13), we further have

$$\limsup_{k \rightarrow \infty} \mathbf{e}_k \leq \frac{3y_-^2 \bar{\pi} \alpha^5}{(1 - \sigma_B^2)^4} \mathcal{O} \left( \frac{\ell^4 \sigma^2}{n^2 \mu} \right) + \frac{3y_-^2 \bar{\pi} \alpha^2}{(1 - \sigma_B^2)^4} \mathcal{O} (\sigma^2) + \frac{3y_-^2 y^2 \alpha^2}{(1 - \sigma_B^2)^4} \mathcal{O} \left( \frac{\ell^2 \sigma^2}{\mu^2} \right) + 3y_-^2 y^2 \alpha \mathcal{O} \left( \frac{\sigma^2}{n \mu} \right). \quad (15)$$

and the theorem follows by dropping the higher order term of  $\alpha$  and noting that  $\frac{\ell^2}{\mu^2} \geq 1$ .  $\square$

**Corollary 2.** For all  $k, \exists b \in \mathbb{R}$ , such that  $\mathbb{E} [\|\mathbf{x}_k\|_2^2] \leq b$ .

The proof follows from Theorem 1.

### B. Proof of Theorem 2

Let  $P_k := \mathbb{E} [\|\mathbf{x}_k - B^\infty \mathbf{x}_k\|_\pi^2]$ ,  $Q_k := \mathbb{E} [\|\bar{\mathbf{x}}_k - \mathbf{z}^*\|_2^2]$  and  $R_k := \mathbb{E} [\|\mathbf{w}_k - B^\infty \mathbf{w}_k\|_\pi^2]$ . To show that

$$P_k \leq \frac{\tilde{P}}{(m+k)^2}, \quad Q_k \leq \frac{\tilde{Q}}{(m+k)}, \quad R_k \leq \tilde{R}, \quad (16)$$

for all  $k \geq 0$ , it suffices to show that the R.H.S of (7), with a decaying step-size  $\alpha_k < \left( \frac{1 - \sigma_B^2}{6\ell} \right) \frac{1}{y_- \sqrt{(1 + \sigma_B^2)h}}$ , follows the above bounds. We develop the proof by induction. Consider (7) for  $k = 0$ , i.e.,

$$A_{\alpha_0} \mathbf{t}_0 + H_0 \mathbf{s}_0 + \mathbf{c}$$

with  $\alpha_0 = \frac{\theta}{m}$ , and therefore  $m > \frac{6\ell\theta y_- \sqrt{(1 + \sigma_B^2)h}}{1 - \sigma_B^2}$ , to obtain the following conditions:

$$\tilde{R} \leq \left( \frac{1 - \sigma_B^2}{\theta^2 (1 + \sigma_B^2)} \right) \left( \frac{m^2}{(m+1)^2} - \frac{1 + \sigma_B^2}{2} \right) \tilde{P}, \quad (17a)$$

$$\tilde{Q} \geq \left[ \left( \frac{\theta}{m} + \frac{1}{\mu} \right) \left( \frac{\theta \ell^2 E_1}{mn(\theta\mu - 1)} \right) \tilde{P} + \frac{nm^2 K_1 b + \theta^2 \sigma^2}{n(\theta\mu - 1)} \right], \quad (17b)$$

$$\tilde{R} \geq \frac{6}{1 - \sigma_B^2} \left[ \left( \frac{E_2}{m^2} \right) \tilde{P} + \left( \frac{\theta^2 \ell^4 E_3}{m^3} \right) \tilde{Q} + K_2 b + C_0 \right]. \quad (17c)$$

where  $E_1, E_2, E_3$  are defined in the following. It can be verified, that the above conditions hold if and only if

$$\begin{aligned} \frac{1 - \sigma_B^2}{\theta^2 (1 + \sigma_B^2)} \left( \frac{m^2}{(m+1)^2} - \frac{1 + \sigma_B^2}{2} \right) \tilde{P} &> \frac{6}{1 - \sigma_B^2} \left[ \frac{E_2 \tilde{P}}{m^2} + \left( \frac{\theta^2 \ell^4 E_3}{m^3} \right) \left( \frac{\theta}{m} + \frac{1}{\mu} \right) \left( \frac{\theta \ell^2 E_1 \tilde{P}}{mn(\theta\mu - 1)} \right) \right] \\ \frac{(1 - \sigma_B^2)^2}{6\theta^2 (1 + \sigma_B^2)} \left( \frac{1 - \sigma_B^2}{2} - \frac{2m+1}{(m+1)^2} \right) &> \frac{E_2}{m^2} + \left( \frac{\theta^3 \ell^6 E_1 E_3}{m^4 n (\theta\mu - 1)} \right) \left( \frac{\theta}{m} + \frac{1}{\mu} \right) \end{aligned}$$

and  $\tilde{Q} = \max \{mQ_0, D_6\}$ , where  $\tilde{P}$  and  $\tilde{R}$  follow the constraints in (17a), (17c), and  $\tilde{R} > R_0$ . We use  $\mathbb{E}\|\mathbf{x}_k\|_2^2 < b$ , for some  $b > 0$ , which follows from Theorem 1. Thus,  $\tilde{P}$  is selected as  $\tilde{P} = \max \left\{ m^2 P_0, \frac{R_0}{D_1}, \frac{D_3}{D_1 - D_2}, \frac{D_5}{D_1 - D_4} \right\}$ , where

$$\begin{aligned} C_0 &:= 4\sigma^2 q \pi^{-1} \left( n + 3 \left( \frac{\theta^2 \ell^2 y^4 y^2}{m^2} \right) \left( \frac{2m^2 k_1 - 3k_2 \theta^2}{m^2 k_1 - 2k_2 \theta^2} \right) \right), & D_2 &:= \frac{6E_2}{m^2(1-\sigma_B^2)}, \\ D_1 &:= \left( \frac{1-\sigma_B^2}{\theta^2(1+\sigma_B^2)} \right) \left( \frac{1-\sigma_B^2}{2} - \frac{2m+1}{(m+1)^2} \right), & D_4 &:= \left[ \frac{6E_1}{1-\sigma_B^2} \right] \left( \frac{\theta^3 \ell^6 E_3}{m^4 n(\theta\mu-1)} \right) \left( \frac{\theta}{m} + \frac{1}{\mu} \right) + D_2, \\ D_3 &:= \left[ \frac{6}{1-\sigma_B^2} \right] \left[ \left( \frac{\theta^2 \ell^4 E_3}{m^3} \right) \|\bar{\mathbf{x}}_0 - \mathbf{z}^*\|_2^2 + C_0 + K_2 b \right], & E_1 &:= (1 + \beta \sigma_B) y_-^2 \bar{\pi}, \\ D_5 &:= \left[ \frac{6}{1-\sigma_B^2} \right] \left[ \left( \frac{\theta^2 \ell^4 E_3}{m^3 n(\theta\mu-1)} \right) (\theta^2 \sigma^2 + nm^2 K_1 b) + C_0 + K_2 b \right], & E_3 &:= 18qy_-^4 y^2 \pi^{-1}, \\ D_6 &:= \left[ \frac{1}{n(\theta\mu-1)} \right] \left[ \left( \frac{\theta}{m} + \frac{1}{\mu} \right) \left( \frac{\theta \ell^2 E_1}{m} \right) \tilde{P} + \theta^2 \sigma^2 + nm^2 K_1 b \right], & K_1 &:= K_3 \left( \frac{\theta \ell^2}{\mu m} + \frac{\theta^2 \ell^2}{m^2} \right), \\ K_2 &:= \frac{12\ell^2 q y_-^4 \beta}{\pi} \left( 2\beta + \frac{\theta^2 \ell^2 y^2 y^2 (\beta+1)}{m^2} \left( \frac{2m^2 k_1 - 3k_2 \theta^2}{m^2 k_1 - 2k_2 \theta^2} \right) \right), & K_3 &:= y_-^2 \beta (\beta + 1), \\ E_2 &:= 4k_2 + \left( \frac{2\ell^2 y^2 k_2 \theta^2}{m^2} \right) \left( \frac{2k_1 m^2 - 3k_2 \theta^2}{k_1 m^2 - 2k_2 \theta^2} \right) (1 + \beta \sigma_B). \end{aligned}$$

Thus, we conclude that (16) holds for  $k = 0$  when the corresponding conditions on  $\tilde{P}, \tilde{Q}, \tilde{R}$ , and  $m$  are met. Next, assume that (16) holds for some  $k$ , it can be verified that it automatically holds for  $k + 1$  with the same conditions on  $\tilde{P}, \tilde{Q}, \tilde{R}$ , and  $m$  that are derived for  $k = 0$ .

We next improve  $Q_k$  to establish the network-independence. Pick  $\tilde{S}$  large enough such that  $\forall k \geq \tilde{S}, \sigma_B^k \leq \frac{1}{n(m+k)^2}$ . Then using the decaying step-size in (7), we have

$$Q_{k+1} \leq \left( 1 - \frac{\theta\mu}{m+k} \right) Q_k + \frac{2\theta\ell^2(E_1\tilde{P} + K_3b)}{n\mu(m+k)^3} + \frac{\theta^2\sigma^2}{n(m+k)^2},$$

which leads to

$$Q_k \leq \prod_{t=0}^{k-1} \left( 1 - \frac{\theta\mu}{m+t} \right) Q_0 + \sum_{t=0}^{k-1} \prod_{j=t+1}^{k-1} \frac{m+j-\theta}{m+j} \left[ \frac{2\theta\ell^2(E_1\tilde{P} + K_3b)}{n\mu(m+t)^3} + \frac{\theta^2\sigma^2}{n(m+t)^2} \right], \quad (18)$$

From [17], we have

$$\prod_{t=0}^{k-1} \left( 1 - \frac{\theta\mu}{m+t} \right) \leq \frac{m^{\theta\mu}}{(m+k)^{\theta\mu}}, \quad \prod_{j=t+1}^{k-1} \left( 1 - \frac{\theta\mu}{m+j} \right) \leq \frac{(m+t+1)^{\theta\mu}}{(m+k)^{\theta\mu}};$$

Using the above relations and in (18),

$$\begin{aligned} Q_k &\leq \frac{m^{\theta\mu}}{(m+k)^{\theta\mu}} Q_0 + \frac{4\theta\ell^2(E_1\tilde{P} + K_3b)}{n\mu(m+k)^{\theta\mu}} \sum_{t=0}^{k-1} (m+t)^{\theta\mu-3} + \frac{2\theta^2\sigma^2}{n(m+k)^{\theta\mu}} \sum_{t=0}^{k-1} (m+t)^{\theta\mu-2} \\ &\leq \frac{m^{\theta\mu}}{(m+k)^{\theta\mu}} Q_0 + \frac{4\theta\ell^2(E_1\tilde{P} + K_3b)}{n\mu(m+k)^{\theta\mu}} \int_{t=-1}^k (m+t)^{\theta\mu-3} dt + \frac{2\theta^2\sigma^2}{n(m+k)^{\theta\mu}} \int_{t=-1}^k (m+t)^{\theta\mu-2} dt \\ &\leq \frac{2\theta^2\sigma^2}{n(\theta\mu-1)(m+k)} + \frac{m^{\theta\mu}}{(m+k)^{\theta\mu}} Q_0 + \max \left\{ \frac{4\theta\ell^2(E_1\tilde{P} + K_3b)}{n\mu(\theta\mu-2)(m+k)^2}, \frac{4\theta\ell^2(E_1\tilde{P} + K_3b)(m-1)^{\theta\mu-2}}{n\mu(2-\theta\mu)\mu(m+k)^{\theta\mu}} \right\}, \end{aligned}$$

and the theorem follows by (3) in Lemma 2 and by noting that the  $\frac{1}{(m+k)}$  term in  $Q_k$  is network independent.  $\square$

## V. NUMERICAL SIMULATIONS

In this section, we illustrate **S-ADDOPT** and compare its performance with related algorithms over directed graphs, i.e., **GP** [20], [21], **ADDOPT** [14], [31], and **SGP** [16], [25], [26]. Recall that **GP** and **ADDOPT** are batch algorithms and operate on the entire local batch of data at each node. In other words, the true gradient  $\nabla f_i$  is used at each node to compute the algorithm updates. In contrast, **SGP** and **S-ADDOPT** employ a stochastic gradient  $\nabla \hat{f}_i(\cdot) = \nabla f_{i,s_k^i}(\cdot)$ , where  $s_k^i$  is chosen uniformly at random from the index set  $\{1, \dots, m_i\}$  at each node  $i$  and each time  $k$ . It can be verified that this choice of stochastic gradient satisfies the SFO setup in Assumption 3. The numerical experiments are described next.

### A. Logistic Regression: Strongly convex

We now show the numerical experiments for a binary classification problem to classify hand-written digits  $\{3, 8\}$  from the MNIST dataset. In this setup, there are a total of  $N = 12,000$  labeled images for training and each node  $i$  possesses a local batch with  $m_i$  training samples. The  $j$ -th sample at node  $i$  is a tuple  $\{\mathbf{x}_{i,j}, y_{i,j}\} \subseteq \mathbb{R}^{784} \times \{+1, -1\}$  and the local logistic regression cost function  $f_i$  at node  $i$  is given by

$$f_i = \frac{1}{m_i} \sum_{j=1}^{m_i} \ln \left[ 1 + \exp \left\{ -(\mathbf{b}^\top \mathbf{x}_{i,j} + c)y_{i,j} \right\} \right] + \frac{\lambda}{2} \|\mathbf{b}\|_2^2,$$

which is smooth and strongly convex because of the addition of the regularizer  $\lambda$ . The nodes cooperate to solve the following decentralized optimization problem:

$$\min_{\mathbf{b} \in \mathbb{R}^{784}, c \in \mathbb{R}} F(\mathbf{b}, c) = \frac{1}{n} \sum_i f_i.$$

For all algorithms, the step-sizes are hand-tuned for best performance. The column stochastic weights are chosen such that  $b_{ji} = |\mathcal{N}_i^{\text{out}}|^{-1}$ , for each  $j \in \mathcal{N}_i^{\text{out}}$ .

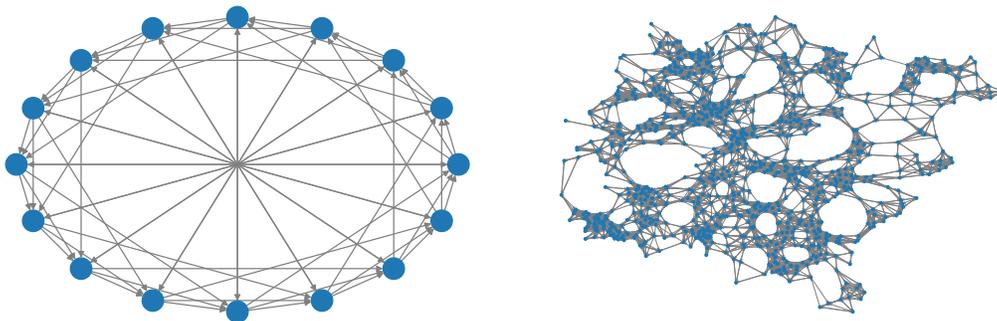


Fig. 1. (Left) Directed exponential graph with  $n = 16$  nodes. (Right) geometric graph with  $n = 1000$  nodes

**Structured training setup–Data-centers:** We choose an exponential graph with  $n = 16$  nodes (Fig. 1, left) to model a highly structured communication graph mimicking, for example, a data center where the data is typically evenly divided among the nodes. In particular, we choose  $m_i = N/n = 750$  training images at each node  $i$ . Performance comparison is provided in Fig. 2, for a constant step-size, and in Fig. 4 (left), for decaying step-sizes,

where we plot the optimality gap  $F(\bar{\mathbf{x}}_k) - F(\mathbf{z}^*)$  versus the number of epochs. Each epoch represents  $N/n = 750$  stochastic gradient evaluations implemented (in parallel) at each node. Recall that **S-ADDOPT** adds gradient tracking to **SGP** and in this balanced data scenario, its performance is virtually indistinguishable from **SGP**, while their batch counterparts are much slower. **ADDOPT** however converges linearly to the exact solution as can be observed in Fig. 2 (right) over a longer number of epochs.

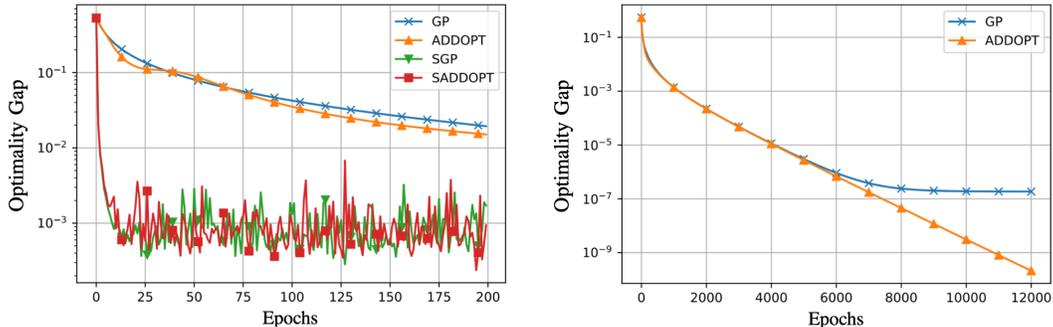


Fig. 2. (Left) Balanced data and constant step-sizes for all algorithms: Performance comparison over the exponential graph with  $n = 16$  nodes and  $m = 750$  data samples per node. (Right) Linear convergence of **ADDOPT** shown over a longer number of epochs.

**Ad hoc training setup–Multi-agent networks:** We next consider a large-scale nearest-neighbor (geometric) digraph with  $n = 1,000$  nodes (Fig. 1, right) that models, for example, ad hoc wireless multi-agent networks, where the agents typically possess different sizes of local batches depending on their locations and local resources; see Fig. 3 (left) for an arbitrary data distribution across the agents. Performance comparison is shown in Fig. 3 (right), for a constant step-size, and in Fig. 4 (right), for decaying step-sizes. Each epoch represents  $N/n = 12$  component gradient evaluations (in parallel) at each node. When the data is unbalanced, the addition of gradient tracking in **S-ADDOPT** results in a significantly improved performance than **SGP**.

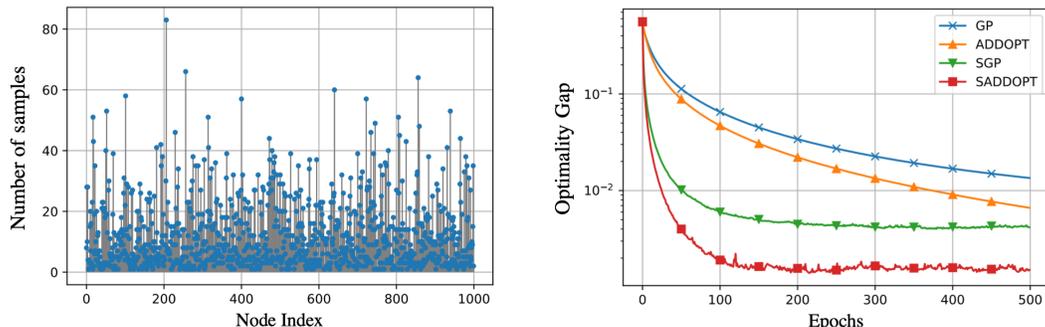


Fig. 3. Performance comparison (right), over the directed geometric graph in Fig. 1 (right), with an unbalanced data distribution (left) and constant step-sizes for all algorithms.

Comparing the structured and ad hoc training scenarios, we note that gradient tracking does not show a noticeable improvement over the balanced data scenario but results in a superior performance when the data distribution is unbalanced. This is because the convergence (15) of **S-ADDOPT** (similar to its undirected counterpart [12]) does not depend on the heterogeneity of local data batches as opposed to **SGP**. A detailed discussion along these lines

can be found in [19].

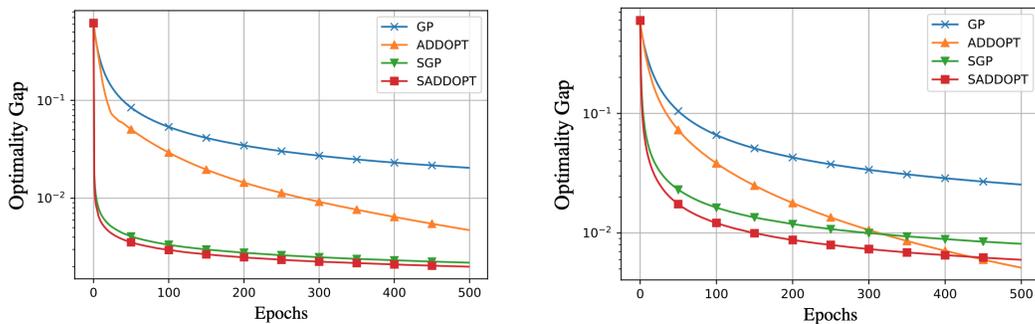


Fig. 4. Performance comparison for exact convergence (decaying step-sizes for **S-ADDOPT** and **SGP**, and constant step-size for **ADDOPT**): (Left) Directed exponential graph with balanced data. (Right) Directed geometric graph with unbalanced data.

### B. Neural networks: Non-convex

Finally, we compare the performance of the stochastic algorithms discussed in this report for training a distributed neural network optimizing a non-convex problem with constant step-sizes of the algorithms. Each node has a local neural network comprising of one fully connected hidden layer of 64 neurons learning 51,675 parameters. We train the neural network to for a multi-class classification problem to classify ten classes in MNIST  $\{0, \dots, 9\}$  and CIFAR-10  $\{\text{“airplanes”}, \dots, \text{“trucks”}\}$  datasets. Both have 60,000 images in total and 6,000 images per class. The data samples are divided randomly and equally over a 500 node directed geometric graph shown in Fig. 5. We

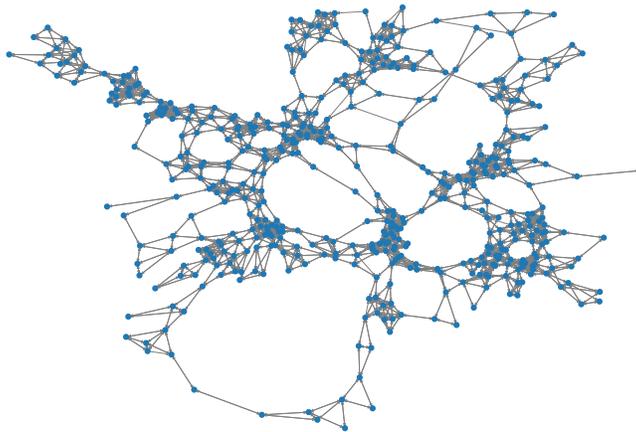


Fig. 5. Directed geometric graph with  $n = 500$  nodes.

show the loss  $F(\bar{\mathbf{x}}_k)$  and test accuracy of **SGP** and **S-ADDOPT** with respect to epochs over the MNIST dataset in Fig. 6. Similarly, Fig. 7 illustrates the performance for the CIFAR-10 dataset. We observe that adding gradient tracking in **SGP** improves the transient and steady state performance in these non-convex problems.

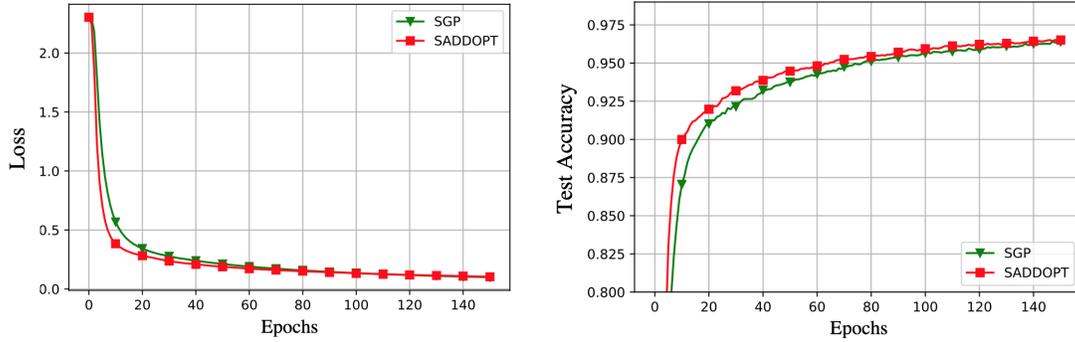


Fig. 6. MNIST classification using a two-layer neural network over a directed geometric graph with  $n = 500$  nodes and  $m = 120$  data samples per node; both algorithms use a constant step-size.

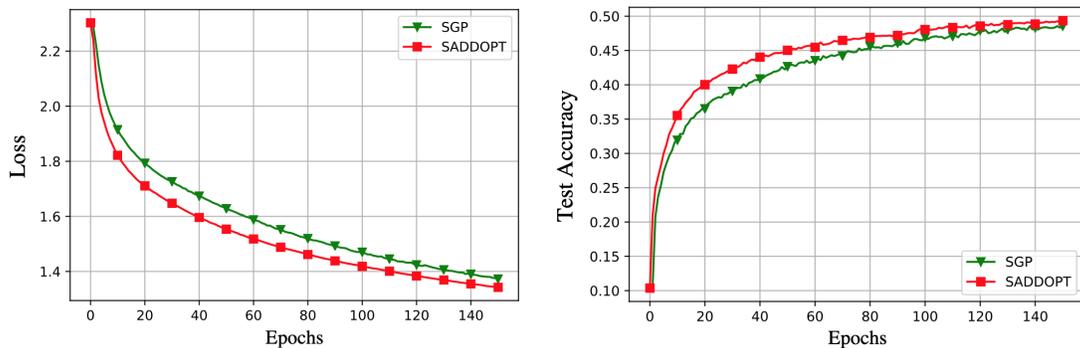


Fig. 7. CIFAR-10 classification using a two-layer neural network over a directed geometric graph with  $n = 500$  nodes and  $m = 120$  data samples per node; both algorithms use a constant step-size.

## VI. CONCLUSIONS

In this report, we present **S-ADDOPT**, a decentralized stochastic optimization algorithm that is applicable to both undirected and directed graphs. **S-ADDOPT** adds gradient tracking to **SGP** and can be viewed as a stochastic extension of **ADDOPT**. We show that for a constant step-size  $\alpha$ , **S-ADDOPT** converges linearly inside an error ball around the optimal, the size of which is controlled by  $\alpha$ . For decaying step-sizes  $\mathcal{O}(1/k)$ , we show that **S-ADDOPT** is asymptotically network-independent and reaches the exact solution sublinearly at  $\mathcal{O}(1/k)$ . These characteristics match the centralized **SGD** up to some constant factors. Numerical experiments over both strongly convex and non-convex problems illustrate the convergence behavior and the performance comparison of **S-ADDOPT** versus **SGP** and their non-stochastic counterparts.

## REFERENCES

- [1] S. Lee and M. M. Zavlanos, "Approximate projection methods for decentralized optimization with functional constraints," *IEEE Transactions on Automatic Control*, vol. 63, no. 10, pp. 3248–3260, Oct. 2018.
- [2] S. Safavi, U. A. Khan, S. Kar, and J. M. F. Moura, "Distributed localization: A linear theory," *Proceedings of the IEEE*, vol. 106, no. 7, pp. 1204–1223, Jul. 2018.
- [3] P. A. Forero, A. Cano, and G. B. Giannakis, "Consensus-based distributed support vector machines," *Journal of Machine Learning Research*, vol. 11, pp. 1663–1707, 2010.

- [4] H. Raja and W. U. Bajwa, “Cloud  $K$ -SVD: A collaborative dictionary learning algorithm for big, distributed data,” *IEEE Transactions on Signal Processing*, vol. 64, no. 1, pp. 173–188, Jan. 2016.
- [5] T. Yang, X. Yi, J. Wu, Y. Yuan, D. Wu, Z. Meng, Y. Hong, H. Wang, Z. Lin, and K. H. Johansson, “A survey of distributed optimization,” *Annual Reviews in Control*, vol. 47, pp. 278 – 305, 2019.
- [6] L. Bottou, F. E. Curtis, and J. Nocedal, “Optimization methods for large-scale machine learning,” *SIAM Review*, vol. 60, no. 2, pp. 223–311, 2018.
- [7] A. Nedić and A. Ozdaglar, “Distributed subgradient methods for multi-agent optimization,” *IEEE Transactions on Automatic Control*, vol. 54, no. 1, pp. 48, 2009.
- [8] K. Yuan, Q. Ling, and W. Yin, “On the convergence of decentralized gradient descent,” *SIAM Journal on Optimization*, vol. 26, no. 3, pp. 1835–1854, Sep. 2016.
- [9] S. S. Ram, A. Nedić, and V. V. Veeravalli, “Distributed stochastic subgradient projection algorithms for convex optimization,” *Journal of Optimization Theory and Applications*, vol. 147, no. 3, pp. 516–545, 2010.
- [10] J. Chen and A. H. Sayed, “Diffusion adaptation strategies for distributed optimization and learning over networks,” *IEEE Transactions on Signal Processing*, vol. 60, no. 8, pp. 4289–4305, Aug. 2012.
- [11] R. Xin, U. A. Khan, and S. Kar, “Variance-reduced decentralized stochastic optimization with accelerated convergence,” *arXiv:1912.04230*, 2019.
- [12] S. Pu and A. Nedić, “Distributed stochastic gradient tracking methods,” *Mathematical Programming*, 2020.
- [13] J. Xu, S. Zhu, Y. C. Soh, and L. Xie, “Augmented distributed gradient methods for multi-agent optimization under uncoordinated constant stepsizes,” in *54th IEEE Conference on Decision and Control*. IEEE, 2015, pp. 2055–2060.
- [14] C. Xi, R. Xin, and U. A. Khan, “ADD-OPT: Accelerated distributed directed optimization,” *IEEE Transactions on Automatic Control*, vol. 63, no. 5, pp. 1329–1339, 2017.
- [15] R. Xin and U. A. Khan, “A linear algorithm for optimization over directed graphs with geometric convergence,” *IEEE Control Systems Letters*, vol. 2, no. 3, pp. 315–320, 2018.
- [16] A. Spiridonoff, A. Olshevsky, and I. C. Paschalidis, “Robust asynchronous stochastic gradient-push: Asymptotically optimal and network-independent performance for strongly convex functions,” *Journal of Machine Learning Research*, vol. 21, no. 58, pp. 1–47, 2020.
- [17] S. Pu, A. Olshevsky, and I. C. Paschalidis, “A sharp estimate on the transient time of distributed stochastic gradient descent,” *1906.02702*, 2019.
- [18] S. Pu, A. Olshevsky, and I. C. Paschalidis, “Asymptotic network independence in distributed stochastic optimization for machine learning: Examining distributed and centralized stochastic gradient descent,” *IEEE Signal Processing Magazine*, vol. 37, no. 3, pp. 114–122, 2020.
- [19] R. Xin, S. Kar, and U. A. Khan, “Decentralized stochastic optimization and machine learning,” *IEEE Signal Processing Magazine*, vol. 3, pp. 102–113, May 2020.
- [20] K. I. Tsianos, S. Lawlor, and M. G. Rabbat, “Push-sum distributed dual averaging for convex optimization,” in *51st IEEE Annual Conference on Decision and Control*, Maui, Hawaii, Dec. 2012, pp. 5453–5458.
- [21] A. Nedić and A. Olshevsky, “Distributed optimization over time-varying directed graphs,” *IEEE Transactions on Automatic Control*, vol. 60, no. 3, pp. 601–615, 2014.
- [22] C. Xi and U. A. Khan, “DEXTRA: A fast algorithm for optimization over directed graphs,” *IEEE Transactions on Automatic Control*, vol. 62, no. 10, pp. 4980–4993, Oct. 2017.
- [23] C. Xi, V. S. Mai, R. Xin, E. Abed, and U. A. Khan, “Linear convergence in optimization over directed graphs with row-stochastic matrices,” *IEEE Transactions on Automatic Control*, vol. 63, no. 10, pp. 3558–3565, Oct. 2018.
- [24] R. Xin, C. Xi, and U. A. Khan, “FROSTFast row-stochastic optimization with uncoordinated step-sizes,” *EURASIP Journal on Advances in Signal Processing*, Jan. 2019.

- [25] A. Nedić and A. Olshevsky, “Stochastic gradient-push for strongly convex functions on time-varying directed graphs,” *IEEE Transactions on Automatic Control*, vol. 61, no. 12, pp. 3936–3947, 2016.
- [26] M. Assran, N. Loizou, N. Ballas, and M. Rabbat, “Stochastic gradient push for distributed deep learning,” in *36th International Conference on Machine Learning*. Jun. 2019, vol. 97, pp. 344–353, PMLR.
- [27] R. Xin, A. K. Sahu, U. A. Khan, and S. Kar, “Distributed stochastic optimization with gradient tracking over strongly-connected networks,” in *58th IEEE Conference on Decision and Control*, Dec. 2019, pp. 8353–8358.
- [28] D. Kempe, A. Dobra, and J. Gehrke, “Gossip-based computation of aggregate information,” in *44th Annual IEEE Symposium on Foundations of Computer Science*, Oct. 2003, pp. 482–491.
- [29] C. Xi and U. A. Khan, “Distributed subgradient projection algorithm over directed graphs,” *IEEE Transactions on Automatic Control*, vol. 62, no. 8, pp. 3986–3992, Oct. 2016.
- [30] C. Xi, Q. Wu, and U. A. Khan, “On the distributed optimization over directed networks,” *Neurocomputing*, vol. 267, pp. 508–515, Dec. 2017.
- [31] A. Nedić, A. Olshevsky, and W. Shi, “Achieving geometric convergence for distributed optimization over time-varying graphs,” *SIAM Journal on Optimization*, vol. 27, no. 4, pp. 2597–2633, 2017.
- [32] R. A. Horn and C. R. Johnson, *Matrix Analysis*, Cambridge University Press, Cambridge, 1985.
- [33] M. Zhu and S. Martínez, “Discrete-time dynamic average consensus,” *Automatica*, vol. 46, no. 2, pp. 322–329, 2010.
- [34] P. Di Lorenzo and G. Scutari, “NEXT: In-network nonconvex optimization,” *IEEE Transactions on Signal and Information Processing over Networks*, vol. 2, no. 2, pp. 120–136, 2016.

## APPENDIX A

DEVELOPING THE LTI SYSTEM DESCRIBING **S-ADDOPT**

To derive the LTI system described in (7), we first define a few terms:

$$\begin{aligned}\bar{\mathbf{w}}_k &:= \frac{1}{n} \mathbf{1}_n^\top \mathbf{w}_k, & \bar{\mathbf{h}}_k &:= \frac{1}{n} \mathbf{1}_n^\top \nabla f(\mathbf{z}_k), & \bar{\mathbf{g}}_k &:= \frac{1}{n} \mathbf{1}_n^\top \nabla \hat{f}(\mathbf{z}_k) := \bar{\mathbf{w}}_k, \\ \bar{\mathbf{p}}_k &:= \frac{1}{n} \mathbf{1}_n^\top \nabla f(\mathbf{1}_n \bar{\mathbf{x}}_k), & \nabla f(\mathbf{z}_k) &:= [\nabla f_1(\mathbf{z}_k^1)^\top, \dots, \nabla f_n(\mathbf{z}_k^n)^\top]^\top.\end{aligned}$$

We denote  $\xi_k^i \in \mathbb{R}^p$  as random vectors for all  $k \geq 0$  and  $i \in \mathcal{V}$  such that the stochastic gradient is  $\nabla \hat{f}_i(\mathbf{z}_k^i) = \nabla f_i(\mathbf{z}_k^i, \xi_k^i)$ . Assumption 3 allows the gradient noise processes to be dependent on agent  $i$  and the current iterate  $\mathbf{z}_k^i$ . We denote by  $\mathcal{F}_k$ , the  $\sigma$ -algebra generated by the set of random vectors  $\{\xi_l^i\}_{i \in \mathcal{V}}$ , where  $0 \leq l \leq k-1$ . The derivation of the system described in (7) is now provided in the following three steps:

**Step 1. Network agreement error.**

Note that the first term  $\|\mathbf{x}_{k+1} - B^\infty \mathbf{x}_{k+1}\|_\pi^2$  in the LTI system is essentially the network agreement error and it can be expanded as:

$$\begin{aligned}\|\mathbf{x}_{k+1} - B^\infty \mathbf{x}_{k+1}\|_\pi^2 &= \|B\mathbf{x}_k - B^\infty \mathbf{x}_k - \alpha(\mathbf{w}_k - B^\infty \mathbf{w}_k)\|_\pi^2 \\ &= \|B\mathbf{x}_k - B^\infty \mathbf{x}_k\|_\pi^2 + \alpha^2 \|\mathbf{w}_k - B^\infty \mathbf{w}_k\|_\pi^2 - 2\langle B\mathbf{x}_k - B^\infty \mathbf{x}_k, \alpha(\mathbf{w}_k - B^\infty \mathbf{w}_k) \rangle_\pi \\ &\leq \sigma_B^2 \|\mathbf{x}_k - B^\infty \mathbf{x}_k\|_\pi^2 + \alpha^2 \|\mathbf{w}_k - B^\infty \mathbf{w}_k\|_\pi^2 + 2\alpha\sigma_B \|\mathbf{x}_k - B^\infty \mathbf{x}_k\|_\pi \|\mathbf{w}_k - B^\infty \mathbf{w}_k\|_\pi \\ &\leq \left( \sigma_B^2 + \alpha\sigma_B \frac{1 - \sigma_B^2}{2\alpha\sigma_B} \right) \|\mathbf{x}_k - B^\infty \mathbf{x}_k\|_\pi^2 + \left( \alpha^2 + \alpha\sigma_B \frac{2\alpha\sigma_B}{1 - \sigma_B^2} \right) \|\mathbf{w}_k - B^\infty \mathbf{w}_k\|_\pi^2 \\ &= \left( \frac{1 + \sigma_B^2}{2} \right) \|\mathbf{x}_k - B^\infty \mathbf{x}_k\|_\pi^2 + \alpha^2 \left( \frac{1 + \sigma_B^2}{1 - \sigma_B^2} \right) \|\mathbf{w}_k - B^\infty \mathbf{w}_k\|_\pi^2.\end{aligned}\tag{19}$$

**Step 2. Optimality gap.**

Next, we consider  $\|\bar{\mathbf{x}}_{k+1} - \mathbf{z}^*\|_2^2$ , which defines the the gap between the mean iterate and the true solution:

$$\|\bar{\mathbf{x}}_{k+1} - \mathbf{z}^*\|_2^2 = \|(\bar{\mathbf{x}}_k - \alpha\bar{\mathbf{w}}_k) - \mathbf{z}^*\|_2^2 = \|\bar{\mathbf{x}}_k - \mathbf{z}^*\|_2^2 + \alpha^2 \|\bar{\mathbf{g}}_k\|_2^2 - 2\langle \bar{\mathbf{x}}_k - \mathbf{z}^*, \bar{\mathbf{g}}_k \rangle.$$

Noticing that  $\mathbb{E}[\bar{\mathbf{g}}_k | \mathcal{F}_k] = \bar{\mathbf{h}}_k$ ,

$$\mathbb{E}[\|\bar{\mathbf{g}}_k\|_2^2 | \mathcal{F}_k] = \mathbb{E}[\|\bar{\mathbf{g}}_k - \bar{\mathbf{h}}_k\|_2^2 | \mathcal{F}_k] + \|\bar{\mathbf{h}}_k\|_2^2 \leq \frac{\sigma^2}{n} + \|\bar{\mathbf{h}}_k\|_2^2.$$

For  $\eta = (1 - \alpha\mu)$ , we can write:

$$\begin{aligned}\mathbb{E}[\|\bar{\mathbf{x}}_{k+1} - \mathbf{z}^*\|_2^2 | \mathcal{F}_k] &\leq \|\bar{\mathbf{x}}_k - \mathbf{z}^*\|_2^2 - 2\langle \bar{\mathbf{x}}_k - \mathbf{z}^*, \bar{\mathbf{h}}_k \rangle + \alpha^2 \|\bar{\mathbf{h}}_k\|_2^2 + \frac{\alpha^2 \sigma^2}{n} \\ &= \|\bar{\mathbf{x}}_k - \mathbf{z}^*\|_2^2 - 2\alpha \langle \bar{\mathbf{x}}_k - \mathbf{z}^*, \bar{\mathbf{p}}_k \rangle + 2\alpha \langle \bar{\mathbf{x}}_k - \mathbf{z}^*, \bar{\mathbf{p}}_k - \bar{\mathbf{h}}_k \rangle + \alpha^2 \|\bar{\mathbf{p}}_k - \bar{\mathbf{h}}_k\|_2^2 \\ &\quad + \alpha^2 \|\bar{\mathbf{p}}_k\|_2^2 - 2\alpha^2 \langle \bar{\mathbf{p}}_k, \bar{\mathbf{p}}_k - \bar{\mathbf{h}}_k \rangle + \frac{\alpha^2 \sigma^2}{n} \\ &= \|\bar{\mathbf{x}}_k - \alpha\bar{\mathbf{p}}_k - \mathbf{z}^*\|_2^2 + \alpha^2 \|\bar{\mathbf{p}}_k - \bar{\mathbf{h}}_k\|_2^2 + 2\alpha \langle \bar{\mathbf{x}}_k - \alpha\bar{\mathbf{p}}_k - \mathbf{z}^*, \bar{\mathbf{p}}_k - \bar{\mathbf{h}}_k \rangle + \frac{\alpha^2 \sigma^2}{n} \\ &\leq \eta^2 \|\bar{\mathbf{x}}_k - \mathbf{z}^*\|_2^2 + \alpha^2 \|\bar{\mathbf{p}}_k - \bar{\mathbf{h}}_k\|_2^2 + 2\alpha\eta \|\bar{\mathbf{x}}_k - \mathbf{z}^*\|_2 \|\bar{\mathbf{p}}_k - \bar{\mathbf{h}}_k\|_2 + \frac{\alpha^2 \sigma^2}{n} \\ &\leq (1 - \alpha\mu) \|\bar{\mathbf{x}}_k - \mathbf{z}^*\|_2^2 + \left( \frac{\alpha\ell^2}{n\mu} \right) (1 + \alpha\mu) \|\mathbf{1}_n \bar{\mathbf{x}}_k - \mathbf{z}_k\|_2^2 + \frac{\alpha^2 \sigma^2}{n}.\end{aligned}\tag{20}$$

It can be verified that  $B^\infty = \frac{1}{n}Y^\infty \mathbf{1}_n \mathbf{1}_n^\top$ . Next consider  $\|\mathbf{z}_k - \mathbf{1}_n \bar{\mathbf{x}}_k\|_2^2$ :

$$\begin{aligned}
\|\mathbf{z}_k - \mathbf{1}_n \bar{\mathbf{x}}_k\|_2^2 &= \|Y^{-1} \mathbf{x}_k - Y^\infty \mathbf{1}_n \bar{\mathbf{x}}_k + Y^\infty \mathbf{1}_n \bar{\mathbf{x}}_k - \mathbf{1}_n \bar{\mathbf{x}}_k\|_2^2 \\
&= \|Y^{-1}(\mathbf{x}_k - Y^\infty \mathbf{1}_n \bar{\mathbf{x}}_k) + (Y^{-1}Y^\infty - I_n) \mathbf{1}_n \bar{\mathbf{x}}_k\|_2^2 \\
&= \|Y^{-1}(\mathbf{x}_k - B^\infty \mathbf{x}_k)\|_2^2 + \|(Y^{-1}Y^\infty - I_n) \mathbf{1}_n \bar{\mathbf{x}}_k\|_2^2 + 2\langle Y^{-1}(\mathbf{x}_k - B^\infty \mathbf{x}_k), (Y^{-1}Y^\infty - I_n) \mathbf{1}_n \bar{\mathbf{x}}_k \rangle \\
&\leq y_-^2 \|\mathbf{x}_k - B^\infty \mathbf{x}_k\|_2^2 + (y_- \beta \sigma_B^k)^2 \|\mathbf{x}_k\|_2^2 + 2(y_-)(y_- \beta \sigma_B^k) \|\mathbf{x}_k - B^\infty \mathbf{x}_k\|_2 \|\mathbf{x}_k\|_2 \\
&\leq (y_-^2 + y_-^2 \beta \sigma_B) \bar{\pi} \|\mathbf{x}_k - B^\infty \mathbf{x}_k\|_\pi^2 + \left( y_-^2 \beta^2 \sigma_B^{2k} + y_-^2 \beta \sigma_B^k \right) \|\mathbf{x}_k\|_2^2.
\end{aligned}$$

Using the above relation in (20), we obtain the final expression for  $\mathbb{E} [\|\bar{\mathbf{x}}_{k+1} - \mathbf{z}^*\|_2^2 | \mathcal{F}_k]$ .

$$\begin{aligned}
\mathbb{E} [\|\bar{\mathbf{x}}_{k+1} - \mathbf{z}^*\|_2^2 | \mathcal{F}_k] &\leq (\alpha^2 g_1 + \alpha g_2) \|\mathbf{x}_k - B^\infty \mathbf{x}_k\|_\pi^2 + (1 - \alpha \mu) \|\bar{\mathbf{x}}_k - \mathbf{z}^*\|_2^2 \\
&\quad + \alpha^2 \left( \frac{\sigma^2}{n} \right) + (h_1 \sigma_B^k) \|\mathbf{x}_k\|_2^2.
\end{aligned} \tag{21}$$

**Step 3: Gradient tracking error.** Finally, we calculate the gradient tracking error  $\|\mathbf{w}_{k+1} - B^\infty \mathbf{w}_{k+1}\|_\pi^2$ .

$$\begin{aligned}
\|\mathbf{w}_{k+1} - B^\infty \mathbf{w}_{k+1}\|_\pi^2 &= \|B \mathbf{w}_k - B^\infty \mathbf{w}_k + (I_n - B^\infty)(\nabla \hat{f}(\mathbf{z}_{k+1}) - \nabla \hat{f}(\mathbf{z}_k))\|_\pi^2 \\
&\leq \sigma_B^2 \|\mathbf{w}_k - B^\infty \mathbf{w}_k\|_\pi^2 + \|(I_n - B^\infty)\|_\pi^2 \|\nabla \hat{f}(\mathbf{z}_{k+1}) - \nabla \hat{f}(\mathbf{z}_k)\|_\pi^2 \\
&\quad + 2\sigma_B \langle \mathbf{w}_k - B^\infty \mathbf{w}_k, (I_n - B^\infty)(\nabla \hat{f}(\mathbf{z}_{k+1}) - \nabla \hat{f}(\mathbf{z}_k)) \rangle_\pi \\
&\leq \sigma_B^2 \|\mathbf{w}_k - B^\infty \mathbf{w}_k\|_\pi^2 + \|\nabla \hat{f}(\mathbf{z}_{k+1}) - \nabla \hat{f}(\mathbf{z}_k)\|_\pi^2 \\
&\quad + 2\sigma_B \|\mathbf{w}_k - B^\infty \mathbf{w}_k\|_\pi \|(I_n - B^\infty)\|_\pi \|\nabla \hat{f}(\mathbf{z}_{k+1}) - \nabla \hat{f}(\mathbf{z}_k)\|_\pi \\
&\leq \left( \sigma_B^2 + \sigma_B \frac{1 - \sigma_B^2}{2\sigma_B} \right) \|\mathbf{w}_k - B^\infty \mathbf{w}_k\|_\pi^2 + \left( 1 + \sigma_B \frac{2\sigma_B}{1 - \sigma_B^2} \right) \|\nabla \hat{f}(\mathbf{z}_{k+1}) - \nabla \hat{f}(\mathbf{z}_k)\|_\pi^2 \\
&= \left( \frac{1 + \sigma_B^2}{2} \right) \|\mathbf{w}_k - B^\infty \mathbf{w}_k\|_\pi^2 + \left( \frac{1 + \sigma_B^2}{1 - \sigma_B^2} \right) \|\nabla \hat{f}(\mathbf{z}_{k+1}) - \nabla \hat{f}(\mathbf{z}_k)\|_\pi^2.
\end{aligned}$$

We bound the second term of the above equation as:

$$\begin{aligned}
\|\nabla \hat{f}(\mathbf{z}_{k+1}) - \nabla \hat{f}(\mathbf{z}_k)\|_\pi^2 &= \|\nabla \hat{f}(\mathbf{z}_{k+1}) - \nabla \hat{f}(\mathbf{z}_k) - (\nabla f(\mathbf{z}_{k+1}) - \nabla f(\mathbf{z}_k)) + \nabla f(\mathbf{z}_{k+1}) - \nabla f(\mathbf{z}_k)\|_\pi^2 \\
&\leq 2\ell^2 \bar{\pi}^{-1} \|\mathbf{z}_{k+1} - \mathbf{z}_k\|_2^2 + 2\|\nabla \hat{f}(\mathbf{z}_{k+1}) - \nabla \hat{f}(\mathbf{z}_k) - (\nabla f(\mathbf{z}_{k+1}) - \nabla f(\mathbf{z}_k))\|_\pi^2.
\end{aligned}$$

Consider the first term  $\|\mathbf{z}_{k+1} - \mathbf{z}_k\|_2^2$  of above equation.

$$\begin{aligned}
\|\mathbf{z}_{k+1} - \mathbf{z}_k\|_2^2 &= \|Y_{k+1}^{-1}((B \mathbf{x}_k - \alpha \mathbf{w}_k) - \mathbf{x}_k) + (Y_{k+1}^{-1} - Y_k^{-1}) \mathbf{x}_k\|_2^2 \\
&= \|Y_{k+1}^{-1}(B - I_n) \mathbf{x}_k - \alpha Y_{k+1}^{-1} \mathbf{w}_k + (Y_{k+1}^{-1} - Y_k^{-1}) \mathbf{x}_k\|_2^2 \\
&\leq \|Y_{k+1}^{-1}(B - I_n) \mathbf{x}_k\|_2^2 + \alpha^2 \|Y_{k+1}^{-1} \mathbf{w}_k\|_2^2 + \|(Y_{k+1}^{-1} - Y_k^{-1}) \mathbf{x}_k\|_2^2 + 2\|Y_{k+1}^{-1}(B - I_n) \mathbf{x}_k\|_2 \|\alpha Y_{k+1}^{-1} \mathbf{w}_k\|_2 \\
&\quad + 2\|\alpha Y_{k+1}^{-1} \mathbf{w}_k\|_2 \|(Y_{k+1}^{-1} - Y_k^{-1}) \mathbf{x}_k\|_2 + 2\|Y_{k+1}^{-1}(B - I_n) \mathbf{x}_k\|_2 \|(Y_{k+1}^{-1} - Y_k^{-1}) \mathbf{x}_k\|_2 \\
&\leq \|Y_{k+1}^{-1}(B - I_n) \mathbf{x}_k\|_2^2 + \|\alpha Y_{k+1}^{-1} \mathbf{w}_k\|_2^2 + \|(Y_{k+1}^{-1} - Y_k^{-1}) \mathbf{x}_k\|_2^2 + 2\|Y_{k+1}^{-1}(B - I_n) \mathbf{x}_k\|_2 \|\alpha Y_{k+1}^{-1} \mathbf{w}_k\|_2 \\
&\quad + 2\alpha \|Y_{k+1}^{-1} \mathbf{w}_k\|_2 \|(Y_{k+1}^{-1} - Y_k^{-1}) \mathbf{x}_k\|_2 + 2\|Y_{k+1}^{-1}(B - I_n) \mathbf{x}_k\|_2 \|(Y_{k+1}^{-1} - Y_k^{-1}) \mathbf{x}_k\|_2 \\
&\leq 12y_-^2 \bar{\pi} \|\mathbf{x}_k - B^\infty \mathbf{x}_k\|_\pi^2 + 3\alpha^2 y_-^2 \|\mathbf{w}_k\|_2^2 + 24y_-^4 \beta^2 \sigma_B^{2k} \|\mathbf{x}_k\|_2^2.
\end{aligned}$$

Next we bound  $\|\mathbf{w}_k\|_2^2$ ,

$$\begin{aligned}
\|\mathbf{w}_k\|_2^2 &= \|(\mathbf{w}_k - Y^\infty \mathbf{1}_n \bar{\mathbf{g}}_k) + Y^{-1} Y^\infty \mathbf{1}_n \bar{\mathbf{p}}_k + Y^{-1} Y^\infty (\mathbf{1}_n \bar{\mathbf{g}}_k - \mathbf{1}_n \bar{\mathbf{p}}_k)\|_2^2 \\
&\leq (2+r) \|\mathbf{w}_k - Y^\infty \mathbf{1}_n \bar{\mathbf{w}}_k\|_2^2 + 3 \|Y^{-1} Y^\infty \mathbf{1}_n \bar{\mathbf{p}}_k\|_2^2 + \left(2 + \frac{1}{r}\right) \|Y^{-1} Y^\infty \mathbf{1}_n (\bar{\mathbf{g}}_k - \bar{\mathbf{p}}_k)\|_2^2 \\
&\leq (2+r) \bar{\pi} \|\mathbf{w}_k - B^\infty \mathbf{w}_k\|_\pi^2 + 3 y_-^2 y^2 \ell^2 \|\bar{\mathbf{x}}_k - \mathbf{z}^*\|_2^2 + 2 \left(2 + \frac{1}{r}\right) y_-^2 y^2 n \|\bar{\mathbf{g}}_k - \bar{\mathbf{h}}_k\|_2^2 \\
&\quad + 2 \left(2 + \frac{1}{r}\right) y_-^2 y^2 \ell^2 \|\mathbf{z}_k - \mathbf{1}_n \bar{\mathbf{x}}_k\|_2^2.
\end{aligned}$$

whereas,

$$\mathbb{E}[\|\nabla \hat{f}(\mathbf{z}_{k+1}) - \nabla \hat{f}(\mathbf{z}_k) - (\nabla f(\mathbf{z}_{k+1}) - \nabla f(\mathbf{z}_k))\|_\pi^2 | \mathcal{F}_k] = 2n\sigma^2 \bar{\pi}^{-1}.$$

Pick  $r = \frac{k_1}{k_2 \alpha^2} - 2 = \frac{k_1 - 2k_2 \alpha^2}{k_2 \alpha^2} > 0 \Rightarrow \frac{1}{r} = \frac{k_2 \alpha^2}{k_1 - 2k_2 \alpha^2} > 0$ . This will enforce a constraint on  $\alpha$  such that  $\alpha < \sqrt{\frac{k_1}{2k_2}} = \left(\frac{1 - \sigma_B^2}{6\ell y_-}\right) \sqrt{\frac{\pi}{(1 + \sigma_B^2) \bar{\pi}}}$ . The term  $\|\mathbf{z}_k - \mathbf{1}_n \bar{\mathbf{x}}_k\|_2^2$  is already simplified in solving for the optimality gap. Putting these in above equation and after taking the expectation, the resultant equation for gradient tracking error becomes:

$$\begin{aligned}
\mathbb{E}[\|\mathbf{w}_{k+1} - B^\infty \mathbf{w}_{k+1}\|_\pi^2 | \mathcal{F}_k] &\leq (g_3 + \alpha^2 g_4) \|\mathbf{x}_k - B^\infty \mathbf{x}_k\|_\pi^2 + (\alpha^2 g_5) \|\bar{\mathbf{x}}_k - \mathbf{z}^*\|_2^2 + C_\sigma \\
&\quad + \left(\frac{5 + \sigma_B^2}{6}\right) \mathbb{E}[\|\mathbf{w}_k - B^\infty \mathbf{w}_k\|_\pi^2 | \mathcal{F}_k] + ((h_2 + \alpha^2 h_3) \sigma_B^k) \|\mathbf{x}_k\|_2^2. \quad (22)
\end{aligned}$$

Taking full expectation of (19), (21), and (22) leads to the system dynamics described by the relation in (7).

## APPENDIX B

### PROOF OF COROLLARY 1

We derive the upper bound on the spectral radius of  $A_\alpha$  under the conditions on step-size described in Theorem 1. Using (8) and (9), the characteristic function of  $A_\alpha$  can be calculated as:

$$\begin{aligned}
\det(\lambda I_3 - A_\alpha) &= (\lambda - a_{11})(\lambda - a_{22})(\lambda - a_{33}) - a_{13}a_{31}(\lambda - a_{22}) - a_{13}a_{21}a_{32} \\
&\geq (\lambda - a_{11})(\lambda - a_{22})(\lambda - a_{33}) - a_{13}a_{31}(\lambda - a_{22}) - \frac{1}{\Gamma + 1}(1 - a_{22})[(1 - a_{11})(1 - a_{33}) - a_{13}a_{31}] \\
&\geq (\lambda - a_{11})(\lambda - a_{22})(\lambda - a_{33}) - \frac{1}{\Gamma}(\lambda - a_{22})(1 - a_{11})(1 - a_{33}) \\
&\quad - \frac{\Gamma - 1}{\Gamma(\Gamma + 1)}(1 - a_{11})(1 - a_{22})(1 - a_{33}).
\end{aligned}$$

Since the  $\det(\lambda I - A_\alpha) > 0$  and the  $\det(\max\{a_{11}, a_{22}, a_{33}\}I - A_\alpha) = \det(a_{22}I - A_\alpha) < 0$ , the spectral radius  $\rho(A_\alpha) = (a_{22}, 1)$ . Suppose  $\lambda = 1 - \epsilon$  for some  $\epsilon \in (0, \alpha\mu)$ , satisfying

$$\begin{aligned}
\det(\lambda I_3 - A_\alpha) &\geq \left(1 - \epsilon - \frac{1 + \sigma_B^2}{2}\right) (\alpha\mu - \epsilon) \left(1 - \epsilon - \frac{5 + \sigma_B^2}{6}\right) - \frac{1}{\Gamma} (\alpha\mu - \epsilon) \left(1 - \frac{1 + \sigma_B^2}{2}\right) \left(1 - \frac{5 + \sigma_B^2}{6}\right) \\
&\quad - \frac{\Gamma - 1}{\Gamma(\Gamma + 1)} \left(1 - \frac{1 + \sigma_B^2}{2}\right) (\alpha\mu) \left(1 - \frac{5 + \sigma_B^2}{6}\right) \geq 0, \\
\iff \left(\frac{1 - \sigma_B^2 - 2\epsilon}{2}\right) (\alpha\mu - \epsilon) \left(\frac{1 - \sigma_B^2 - 6\epsilon}{6}\right) - \frac{1}{\Gamma} (\alpha\mu - \epsilon) \left(\frac{1 - \sigma_B^2}{2}\right) \left(\frac{1 - \sigma_B^2}{6}\right) \\
&\quad - \frac{\Gamma - 1}{\Gamma(\Gamma + 1)} \left(\frac{1 - \sigma_B^2}{2}\right) (\alpha\mu) \left(\frac{1 - \sigma_B^2}{6}\right) \geq 0, \\
\iff (\alpha\mu - \epsilon) \left[ (1 - \sigma_B^2 - 2\epsilon)(1 - \sigma_B^2 - 6\epsilon) - \frac{1}{\Gamma} (1 - \sigma_B^2)^2 \right] &\geq \frac{\Gamma - 1}{\Gamma(\Gamma + 1)} (1 - \sigma_B^2)^2 (\alpha\mu), \\
\iff \left(\frac{\alpha\mu - \epsilon}{\alpha\mu}\right) \left[ \frac{(1 - \sigma_B^2 - 2\epsilon)(1 - \sigma_B^2 - 6\epsilon)}{(1 - \sigma_B^2)^2} - \frac{1}{\Gamma} \right] &\geq \frac{\Gamma - 1}{\Gamma(\Gamma + 1)}. \tag{23}
\end{aligned}$$

It is sufficient to have

$$\epsilon \leq \left(\frac{\Gamma - 1}{\Gamma + 1}\right) \alpha\mu.$$

Notice that,

$$\left(\frac{\alpha\mu - \epsilon}{\alpha\mu}\right) \geq \left(\frac{\alpha\mu - \left(\frac{\Gamma - 1}{\Gamma + 1}\right) \alpha\mu}{\alpha\mu}\right) = 1 - \left(\frac{\Gamma - 1}{\Gamma + 1}\right) = \frac{\Gamma + 1 - \Gamma + 1}{\Gamma + 1} = \frac{2}{\Gamma + 1}.$$

To verify the upper bound on  $\epsilon$  under the condition on step-size described in Corollary 1,

$$\epsilon \leq \left(\frac{\Gamma - 1}{\Gamma + 1}\right) \left(\frac{\Gamma + 1}{\Gamma}\right) \left(\frac{1 - \sigma_B^2}{20\mu}\right) \mu = \left(\frac{\Gamma - 1}{\Gamma}\right) \left(\frac{1 - \sigma_B^2}{20}\right),$$

which implies,

$$\begin{aligned}
1 - \sigma_B^2 - 2\epsilon &\geq 1 - \sigma_B^2 - 2 \left(\frac{\Gamma - 1}{\Gamma}\right) \left(\frac{1 - \sigma_B^2}{20}\right) = \frac{(9\Gamma + 1)(1 - \sigma_B^2)}{10\Gamma}, \\
1 - \sigma_B^2 - 6\epsilon &\geq 1 - \sigma_B^2 - 6 \left(\frac{\Gamma - 1}{\Gamma}\right) \left(\frac{1 - \sigma_B^2}{20}\right) = \frac{(7\Gamma + 3)(1 - \sigma_B^2)}{10\Gamma}, \\
\iff (1 - \sigma_B^2 - 2\epsilon)(1 - \sigma_B^2 - 6\epsilon) &\geq \frac{(63\Gamma^2 + 34\Gamma + 3)(1 - \sigma_B^2)^2}{100\Gamma^2}.
\end{aligned}$$

Plugging these values in (23) and for  $\Gamma > 1$ , we get,

$$\begin{aligned}
\left(\frac{\alpha\mu - \epsilon}{\alpha\mu}\right) \left[ \frac{(1 - \sigma_B^2 - 2\epsilon)(1 - \sigma_B^2 - 6\epsilon)}{(1 - \sigma_B^2)^2} - \frac{1}{\Gamma} \right] &\geq \left(\frac{2}{\Gamma + 1}\right) \left[ \frac{(63\Gamma^2 + 34\Gamma + 3)(1 - \sigma_B^2)^2}{100\Gamma^2} - \frac{1}{\Gamma} \right] \\
&= \left(\frac{1}{\Gamma(\Gamma + 1)}\right) \left[ \frac{(63\Gamma^2 + 34\Gamma + 3)}{50\Gamma} - 2 \right] = \left(\frac{1}{\Gamma(\Gamma + 1)}\right) \left[ \frac{63\Gamma^2 - 66\Gamma + 3}{50\Gamma} \right] \\
&= \left(\frac{1}{\Gamma(\Gamma + 1)}\right) \left[ \Gamma - 1 + \frac{13\Gamma}{50} - \frac{16}{50} + \frac{3}{50\Gamma} \right] \geq \frac{\Gamma - 1}{\Gamma(\Gamma + 1)}.
\end{aligned}$$

Define  $\lambda^* = 1 - \left(\frac{\Gamma - 1}{\Gamma + 1}\right) \alpha\mu$ . Then the  $\det(\lambda^* I - A_\alpha) \geq 0$ . Therefore,  $\rho(A_\alpha) \leq \lambda^*$ . We select  $\Gamma = 2$  and the corollary follows.